7-2-2018

Curve Tracking Control Under State Constraints and Uncertainties

Robert Kelly Sizemore
Louisiana State University and Agricultural and Mechanical College, rsizem2@lsu.edu

CURVE TRACKING CONTROL UNDER STATE CONSTRAINTS AND UNCERTAINTIES

A Dissertation

Submitted to the Graduate Faculty of the
Louisiana State University and
Agricultural and Mechanical College
in partial fulfillment of the
requirements for the degree of
Doctor of Philosophy

in

The Department of Mathematics

by
Robert K. Sizemore
B.S. in Math., University of North Carolina at Wilmington, 2010
M.A., Wake Forest University, 2013
August 2018

Acknowledgments

I thank my advisor, Prof. Michael Malisoff, for including me in his research projects and suggesting the problems addressed in my research. Without his guidance, this work would not have been possible. I also thank Prof. Peter Wolenski, whose differential equations lectures sparked my initial interest in this field, and for personally introducing me to Prof. Malisoff in the Summer of 2015. I also thank Prof. Fumin Zhang of Georgia Tech for his preliminary research and guidance that helped provide the foundation for this dissertation, through his work on modeling and experimental implementation of controller designs that are discussed in this work. I also thank the rest of my doctoral committee, Profs. Boris Rubin, Stephen Shipman, and Jiuyi Zhu for their helpful comments and suggestions on my research. This dissertation is based on my joint publications [32, 33] with Profs. Malisoff and Zhang.

Table of Contents

Abstract

We study a class of steering control problems for free-moving particles tracking a curve in the plane and also in a three-dimensional environment, which are central problems in robotics. In the two-dimensional case, we provide adaptive controllers for curve tracking under unknown curvatures and control uncertainty. The system dynamics include a nonlinear dependence on the curvature, and are coupled with an estimator for the unknown curvature to form the augmented error dynamics. This nonlinear dependence puts our curvature identification objective outside the scope of existing adaptive tracking and parameter identification results that were limited to cases where the unknown parameters enter the system in an affine way. We prove input-to-state stability of the augmented error dynamics under polygonal state constraints and under suitable known bounds on the curvature and on the control uncertainty. When the uncertainty is zero, this ensures tracking of the curve and convergence of the curvature estimate to the unknown curvature. In the three-dimensional setting, we provide a new method to achieve curve tracking, identify unknown control gains, and maintain robust forward invariance of compact regions in the state space, under arbitrarily large perturbation bounds. Our new technique entails scaling certain control components.

Chapter 1
Preliminaries on Control Theory

This dissertation is devoted to a class of research problems in control theory. Control theory is a central research area at the interface of applied mathematics and engineering that plays a prominent role in robotics and other engineering applications. Control theory is the study of a class of dynamical systems called control systems, which differ from the standard dynamical systems that arise in the fields of differential equations or dynamical systems theory because control systems contain parameters that are called controls. When control systems are modeled as systems of ordinary differential equations, the controls are state or time dependent parameters in the right hand side that are often used to represent forces that can be applied to the physical system that is being modeled. Then the goal is to find formulas for the controls such that all solutions of the system for a prescribed set of initial conditions have some desired prescribed property, such as asymptotically converging to an equilibrium point or remaining in some desired region of the state space for all times larger than the initial time. The process of finding formulas for controls is called control design. This process must take into account the feasibility of applying the control in the engineering systems that is being modeled.

One branch of control theory is called optimal control, in which the controls are functions of only time, and where the goal is typically to choose controls that minimize a cost criterion, which is usually represented as an integral involving solutions of the systems that correspond to a particular choice of the control; see [7, 46]. Another branch is called feedback control, where the controls generally also depend on the state of the system (but see [36] for an application of control theory in mathematical biology where the controls are constant and where there is no cost criterion being minimized). See [2] for a laypersons' presentation of the basic ideas

feedback control. Feedback controls play an important role in many engineering applications, especially in robotics, where the objective usually entails applying feedback controls to enable the robot to achieve a desired prescribed behavior autonomously or with reduced human intervention.

However, control systems generally involve uncertainty, which can arise from uncertainty about the underlying engineering system that is being modeled by the system of differential equations, or uncertainty about the effects of the control on the engineering system. This gives rise to mathematical models of control systems that contain unknown constant parameters that one may wish to identify (such as unknown control gains, which are often modeled as constants that multiply the control in the control system), or models with unknown time-varying functions (called perturbations or uncertainties) that represent uncertain effects that can change over time. One important framework for identifying unknown parameters in control systems is called adaptive control, which typically entails constructing an additional system of differential equations whose state provides an estimate of the unknown model parameters that converges to the true values of the model parameters over time; see the monographs [4] and [19], and the survey [20].

This dissertation will focus on a class of feedback control design problems for curve tracking systems, and will use adaptive control to identify unknown control gains and unknown curvatures. The systems that we focus on in this dissertation arose in recent research on the use of marine robots to search for residual pollution from the Deepwater Horizon oil spill disaster. While this work will be confined to a mathematical analysis of control theory problems related to curve tracking, the work [40] discusses more applied aspects related to implementing the types of feedback controls that we provide in this dissertation in marine robotic surveys

that searched for pollution from oil spills. This chapter provides preliminaries on control theory that help make our work more self contained.

We will study systems of the form

$$\dot{x}(t) = f(t, x(t), P, u(t, x(t), \hat{P}(t)), \delta(t)) \tag{1.1}$$

having a subset $\mathcal{X}$ of Euclidean space of arbitrary dimension as its state space, where P is a vector of unknown constant parameters, δ is an unknown measurable locally essentially bounded function that can also represent the effects of uncertainty, u represents the control, and $\hat{P}$ is an estimate of the unknown parameter vector P (but see Section 2.6 below for an analog where the unknown P can also be time varying). Systems of the form (1.1) are called adaptive systems. To ensure that solutions of (1.1) are defined for all initial conditions and all choices of δ, one needs to impose regularity conditions on f and u that typically involve variants of the standard Lipschitzness condition and which will be readily checked for the control systems in later chapters below. Since (1.1) has the state space $\mathcal{X}$, all solutions are valued in $\mathcal{X}$ at all times. The function f is assumed to be known.

An important feature of (1.1) is that although the right side of (1.1) depends on the unknown parameter P, the control u is not allowed to depend on P, because one cannot implement a control that depends on an unknown quantity in the engineering system that is being modeled. The estimate $\hat{P}$ is typically modeled as a solution of a system of the form

$$\dot{\hat{P}}(t) = g(t, x(t), \hat{P}(t), \delta(t)) \tag{1.2}$$

which is then called an estimator of P, in which case the control design problem consists of finding formulas for both u and g so that $\hat{P}(t) \to P$ for all choices of the initial conditions for (1.2) and so that the solutions $x(t)$ of (1.1) satisfy other prescribed properties (such as the input-to-state stability condition that we

discuss below). Notice that as in the case of u, the estimator dynamics (1.2) has no dependence on the unknown parameter vector P, which is needed to ensure implementability. One generally also needs to require Lipschitzness or related regularity conditions on g to ensure that $\hat{P}(t)$ is defined for all nonnegative times for all solutions of the estimator dynamics (1.2), which will be satisfied in the systems that we study in future chapters. One strategy that we will find useful later in this dissertation is to use known bounds on the components of the unknown parameter P to help find a formula for the required function g, which will be of the barrier type that was also used in [31] in cases where the unknown parameters to be identified enter in an affine way. This approach is usually feasible in practice, because even if P is not known, one usually knows intervals that contain its components.

The special case of (1.1) where the system does not depend on P and where the control u has already been chosen produces systems of the form

$$\dot{X}(t) = F(t, X(t), \delta(t)) \tag{1.3}$$

which are called closed loop systems, and which are of the type normally encountered in the theory of differential equations. Systems of the form (1.3) often arise when we choose

$$X(t) = (q(t) - q_r(t), \hat{P}(t) - P), \tag{1.4}$$

where q can represent the state of a physical system and q_r is a prescribed function for which one wishes to ensure that $q(t) - q_r(t) \to 0$ as $t \to +\infty$. In that case, we refer to q_r as a reference trajectory and we say that we wish $q(t)$ to track q_r, and the corresponding closed loop system (1.3) obtained this way is called an augmented tracking and parameter estimation dynamics, or the augmented error dynamics, having the equilibrium point 0, and $q(t) - q_r(t)$ is called the tracking error.

For systems of the form (1.3), one often wishes to prove input-to-state stability (or ISS) with respect to δ, which is an analog of uniform global asymptotic stability for systems of the form (1.3) that was introduced by Sontag in [42] in 1989, and which is now discussed in standard nonlinear control texts, e.g., [17, Chapter 4]. For instance, when the state $X(t)$ of (1.3) has the form (1.4), achieving ISS of (1.3) will mean that when δ is the zero function, we have $\lim_{t\to+\infty}(q(t)-q_r(t), \hat{P}(t)-P) = 0$ from all initial conditions, i.e., the state $q(t)$ of the physical system tracks $q_r(t)$ and we have the parameter identification condition that $\hat{P}(t)$ converges to P. We next review the basic ideas of ISS; see [44] for more detailed discussions on ISS. For what follows, we always assume that the initial times for solutions of (1.3) are 0, so we use $X(t, X_0, \delta)$ to denote the unique solution of (1.3) for the initial condition $X(0) = X_0$ for a given choice of X_0 and a given choice of the function δ, which we assume is uniquely defined for all $t \geq 0$ (which will be the case under Lipschitzness conditions that will be satisfied in later chapters).

We first need several preliminary definitions. Let $|\cdot|$ denote the standard Euclidean norm and the induced matrix norm, and $|\phi|_\infty$ (resp., $|\phi|_{\mathcal{I}}$) denote the essential supremum (resp., supremum over any interval $\mathcal{I}$) for any bounded (resp., locally bounded) $\mathbb{R}^n$ valued measurable function ϕ, where we maintain our convention that the dimensions of our Euclidean spaces are arbitrary. We use C^0 to mean continuous. A C^0 function $\gamma : [0, +\infty) \to [0, +\infty)$ is of class $\mathcal{K}$ and write $\gamma \in \mathcal{K}$ provided it is strictly increasing and $\gamma(0) = 0$. It is of class $\mathcal{K}_\infty$ if, in addition, $\gamma(r) \to +\infty$ as $r \to +\infty$. A C^0 function $\beta : [0, +\infty) \times [0, +\infty) \to [0, +\infty)$ belongs to class $\mathcal{KL}$ provided for each fixed $s \geq 0$, the function $\beta(\cdot, s)$ belongs to class $\mathcal{K}$, and for each fixed $r \geq 0$, $\beta(r, \cdot)$ is non-increasing and $\beta(r, s) \to 0$ as $s \to +\infty$.

Next, consider any subset $\mathcal{O}$ of a Euclidean space and any point $\mathcal{E} \in \mathcal{O}$. A continuous function $\mathcal{V} : \mathcal{O} \to [0, +\infty)$ is called *positive semi-definite with respect*

to $\mathcal{E}$ provided $\mathcal{V}(\mathcal{E}) = 0$; if, in addition, $\mathcal{V}(q) > 0$ for all $q \in \mathcal{O} \setminus \{\mathcal{E}\}$, then $\mathcal{V}$ is called *positive definite with respect to* $\mathcal{E}$ (and simply positive definite in the special case where $\mathcal{E} = 0$). A function $\mathcal{V}$ is *negative semi-definite* (resp., *negative definite*) *with respect to* $\mathcal{E}$ provided $-\mathcal{V}$ is positive semi-definite (resp., positive definite) with respect to $\mathcal{E}$. Let $|p|_{\mathcal{E}} = |p - \mathcal{E}|$ denote the distance between any point $p \in \mathcal{O}$ and the point $\mathcal{E}$. We say that $\mathcal{V} : \mathcal{O} \to [0, +\infty)$ is a *modulus with respect to* $(\mathcal{E}, \mathcal{O})$ provided it is positive definite with respect to $\mathcal{E}$ and radially unbounded in this sense: For each constant $M > 0$, there is a constant $\delta_M > 0$ such that $\mathcal{V}(x) \geq M$ for all $x \in \mathcal{O}$ that satisfy either $\text{dist}(x, \text{boundary}(\mathcal{O})) \leq \delta_M$ or $|x|_{\mathcal{E}} \geq 1/\delta_M$, where dist is the usual Hausdorff distance.

Let $\mathcal{U}$ be any subset of a Euclidean space such that $0 \in \mathcal{U}$. Consider a system of the form (1.3) with state space $\mathcal{O}$ and measurable essentially bounded disturbances $\delta : [0, +\infty) \to \mathcal{U}$, where $\mathcal{F} : \mathbb{R} \times \mathcal{O} \times \mathcal{U} \to \mathcal{O}$ satisfies the standard existence and uniqueness of solutions properties and $\mathcal{F}(t, \mathcal{E}, 0) = 0$ for all $t \geq 0$. Let $\mathcal{S} \subseteq \mathcal{O}$ be a neighborhood of $\mathcal{E}$. We say that the system (1.3) is *input-to-state stable (ISS)* with respect to $(\mathcal{U}, \mathcal{E}, \mathcal{S})$ provided there are $\beta \in \mathcal{KL}$ and $\gamma \in \mathcal{K}_\infty$ and a modulus Λ with respect to $(\mathcal{E}, \mathcal{S})$ such that for all $t \geq 0$, we have

$$|X(t, X_0, \delta)|_{\mathcal{E}} \leq \beta(\Lambda(X_0), t) + \gamma(|\delta|_{[0,t]}) \tag{1.5}$$

for all solutions $X(t, X_0, \delta)$ of (1.3) with initial states $X_0 \in \mathcal{S}$, and all $\mathcal{U}$-valued δ's. This agrees with the usual ISS condition from [44] when $\mathcal{O} = \mathcal{S} = \mathbb{R}^n$, $\mathcal{E} = 0$, and $\Lambda(x) = |x|$. When $\mathcal{F}$ only depends on (t, X) and $\gamma(|\delta|_{[0,t]})$ in (1.5) is not present is called *(uniform) global asymptotic stability (GAS)* with respect to $(\mathcal{E}, \mathcal{S})$. We also use ISS to mean input-to-state stability.

Proving GAS for nonlinear systems usually entails Lyapunov function methods, since the existence of a suitable Lyapunov function is a useful sufficient condition

for GAS, and because one cannot in general find explicit expressions for the flow map for nonlinear systems; see, e.g., [14, Chapter 9]. In an analogous way, it is often useful to prove ISS properties indirectly, since the existence of an ISS Lyapunov function is usually sufficient for ISS. For the definition of ISS Lyapunov functions and relationships between ISS and the existence of ISS Lyapunov functions, see [45].

The construction of the required control formula u in (1.1) is generally done by first finding a function u such that

$$\dot{x}(t) = f(t, x(t), P, u(t, x(t), P), \delta(t)) \tag{1.6}$$

satisfies control requirements like ISS, and then replacing P by its estimate $\hat{P}$ in the control. For cases where f is linear and time invariant, one can often find the required function u using linear algebra methods. For instance, if $A \in \mathbb{R}^{n\times n}$ and $B \in \mathbb{R}^{n\times m}$ are constant matrices such that the $n \times nm$ matrix $[B\ AB\ A^2B\ \dots A^{n-1}B]$ has rank n, where the dimensions m and n are arbitrary, then we can use the Pole Shifting Theorem from [43, Chapter 5] to find a constant matrix $K \in \mathbb{R}^{m\times n}$ such that the matrix $H = A + BK$ admits a symmetric positive definite matrix P_* such that $P_*H^\top + HP_*$ is negative definite. This readily implies that $V(x) = x^\top P_* x$ is a strict Lyapunov function for the system $\dot{x} = Hx$, which we can use to show that

$$\dot{x}(t) = Ax(t) + Bu(x(t)) + \delta(t) \tag{1.7}$$

is ISS with respect to $(\mathbb{R}^n, 0, \mathbb{R}^n)$ when we choose $u(x) = Kx$. However, when f contains nonlinearities, or if A and B are time varying, then the Pole Shifting Theorem would not apply. Instead, one can often use other techniques such as those of [17] to find the desired function u.

If one has a formula for a control u_0 such that $\dot{x}(t) = f(t, x(t), P, u_0(t, x(t), P), 0)$ is GAS with respect to $(0, \mathbb{R}^n)$, then it is often possible to transform u_0 to obtain

a new control such that (1.6) is ISS with respect to $(\mathbb{R}^m, 0, \mathbb{R}^n)$. For an example of how this can be done, consider the special case where there is no dependence on P and where the system is time invariant and control affine, i.e., where f has the form $f(x,u) = f_0(x) + g_0(x)u$ for some functions f_0 and g_0, and where one knows a function u_0 such that

$$\dot{x}(t) = f_0(x(t)) + g_0(x(t))u_0(x(t)) \tag{1.8}$$

is GAS with respect to $(0, \mathbb{R}^n)$. Then converse Lyapunov function theory (e.g., from [6]) provides a strict Lyapunov function $V : \mathbb{R}^n \to [0, +\infty)$ for (1.8) and a function $\alpha_0 \in \mathcal{K}_\infty$ such that the time derivative $\dot{V}$ of V along all solutions of (1.8) satisfies $\dot{V} \leq -\alpha_0(|x(t)|)$ for all $t \geq 0$. Then the new control $u(x) = u_0(x) - \nabla V(x) g_0(x)$ is such that

$$\dot{x}(t) = f_0(x(t)) + g_0(x(t))\big(u(x(t)) + \delta(t)\big) \tag{1.9}$$

is ISS with respect to $(\mathbb{R}^m, 0, \mathbb{R}^n)$; see [44]. This follows because the time derivative $\dot{V}$ of V along all solutions of (1.9) satisfies

$$\begin{array}{rcl} \dot{V} & \leq & -\alpha_0(|x(t)|) + \nabla V(x(t)) g_0(x(t)) \big[-\nabla V(x(t)) g_0(x(t)) + \delta(t) \big] \\ & \leq & -\alpha_0(|x(t)|) - \frac{1}{2} |\nabla V(x(t)) g_0(x(t))|^2 + \frac{1}{2} |\delta(t)|^2 \end{array} \tag{1.10}$$

for all $t \geq 0$, by using the triangle inequality to obtain

$$|\nabla V(x(t)) g_0(x(t)) \delta(t)| \leq \frac{1}{2} |\nabla V(x(t)) g_0(x(t))|^2 + \frac{1}{2} |\delta(t)|^2 \tag{1.11}$$

for all $t \geq 0$.

The preceding calculation implies that V is an ISS Lyapunov function for (1.9), the existence of which is sufficient for the desired ISS property for (1.9). This ISS conclusion is useful, because the additive uncertainties on $u(x(t))$ in (1.9) can represent the effects of actuator errors which are commonly encountered in engineering applications [27]. While the preceding control redesign process of transforming u_0

into u is easy to compute, a more difficult problem that we will study in this dissertation will be that of ensuring ISS with respect to additive uncertainties on the given controls (e.g., gyroscopic type controls that are commonly used in robotic applications) without redesigning the control. This problem is of considerable interest in control engineering cases where the preceding control redesign process would not be allowed, and our solutions for this problem will require introducing suitable bounds on the allowable additive uncertainties δ.

We close this chapter by discussing relevant notions of forward invariance. In the basic theory of differential equations for systems of the form

$$\dot{X}(t) = \mathcal{F}(X(t)) \tag{1.12}$$

having a state space $\mathcal{O}$, forward invariance of a set $\mathcal{S} \subseteq \mathcal{O}$ is the requirement that for all initial states $X_0 \in \mathcal{S}$, the corresponding solution of $X(t, X_0)$ is valued in $\mathcal{S}$ for all $t \geq 0$. The following definition (e.g., from [25]) provides an analog of the preceding forward invariance definition for perturbed systems of the form (1.3) having a state space $\mathcal{O}$. A set $\mathcal{H} \subseteq \mathcal{O}$ is called *robustly forwardly invariant for (1.3) with disturbances valued in* $\mathcal{U}$ provided all solutions of (1.3) with initial states in $\mathcal{S}$ for all disturbances δ valued in $\mathcal{U}$ remain in $\mathcal{S}$ for all $t \geq 0$, i.e., $X(t, \mathcal{S}, \delta) \subseteq \mathcal{S}$ for all $t \geq 0$ and all $\mathcal{U}$-valued δ's, which agrees with the strong forward invariance definition from set-valued analysis [5]. The study of robustly forwardly invariant sets is motivated by robotics applications, where the set $\mathcal{S}$ can represent safety and tolerance bounds. For instance, $\mathcal{S}$ can represent a region in which the robot can safely navigate without encountering any obstacles. This is important since robots can be damaged in collisions, and they can be expensive to repair or replace.

In addition to using novel adaptive control methods to identify unknown model parameters, two key ingredients in the results to follow are that we provide new

ISS results while also ensuring robust forward invariance of sets of interest in our state spaces. Our robust forward invariance approach is a novel treatment of state constrained problems where, instead of the usual approach where the state constraint is prescribed by the dynamical systems under study, our state constraint sets are chosen specifically to facilitate finding largest possible disturbance sets $\mathcal{U}$ that ensure the robust forward invariance of the state constraint sets. Then we can decompose the original state space for the dynamics into a nested sequence of robustly forwardly invariant sets, each with a corresponding largest allowable disturbance set, i.e., robust forward invariant decompositions, which are useful for generating tolerance and safety bounds. In the next chapters, we provide our new results.

Chapter 2
Adaptive Planar Curve Tracking

This chapter presents our work [33] on 2D curve tracking, whose novelty involves our ability to identify unknown curvatures while achieving tracking under control uncertainty and ensuring robust forward invariance of suitable regions in a 2D workspace. Since the curvature enters the dynamics in a nonlinear way, such problems present challenges which were beyond the scope of existing adaptive tracking and parameter identification results that were limited to adaptive systems where the unknown parameter enters the system in an affine way. A key ingredient is our decomposition of the state space into a nested sequence of robustly forwardly invariant hexagons that make it possible to compute bounds on the allowable perturbations that ensure desirable robust forward invariance properties.

2.1 Background

This chapter continues our research group's quest (begun in [25], [28], and [31]) for curve tracking controls that ensure key stability properties under uncertainties and state constraints. Curve tracking is important for navigating mobile robots; see [23], [28], and [47]. The work [37] provides feedback controls for wheeled mobile robots which track boundaries of obstacles, based on Frenet-Serret frames; and [1], [9], and [12] provide generalized adaptive robot controllers for under-actuated autonomous ships and other cases. See also [15], [38], and [50].

Using the curve tracking controls from [51] and polygonal state constraints, the work [25] proved robustness of the curve tracking. While experimental evidence of robustness of curve tracking controls had been observed in farming, obstacle avoidance in corridors, ocean sampling, and ship control (in [22], [53], [50], and [13], respectively), the work [25] provided a mathematical analysis based on a new Lyapunov function design and therefore provided theoretical justification for the

experimental observations. In addition to the Lyapunov analysis, a key contribution in [25] was a proof of robust forward invariance of a class of hexagonal regions $H \subseteq \mathbb{R}^2$. For each such H, [25] computed the supremum of the set of all constants $\delta_H > 0$ such that all trajectories starting in H, for all additive (measurable essentially bounded) control uncertainties that are bounded by δ_H, remain in H. By viewing the planar workspace as a nested sequence $\{H_i\}$ of polygonal regions, this gave predictable tolerance and safety bounds by proving ISS of the curve tracking dynamics on each set H_i, under additive uncertainty on the control and maximal perturbation bounds.

The controls from [25] and [51] were implemented in our research group's deployment of marine robots at Grand Isle, Louisiana, which surveyed the long term impacts of the 2010 Deepwater Horizon oil spill; see [40]. Robust forward invariance can incorporate obstacles in marine surveys. The work at Grand Isle tested our group's controls under different control gains, and [28] extended [25] by proving adaptive tracking with identification of control gains. While our group's work does not explicitly take side slip into account, our group's experimental deployments showed good performance of our robust control approach, even if there are no actuators that compensate for side slip. However, [25], [28], and [31] assume that one knows the curvatures along the curves being tracked, which can make the work difficult to apply. For instance, in marine robotic surveys, the boundary curves of our regions of interest (e.g., areas of pollution shortly after an oil spill) may be uncertain. See [10], [11], and [18] for more motivation for adaptiveness.

Therefore, this chapter provides an adaptive controller for curve tracking. The controller uses a strict Lyapunov function from [25]. However, the novel features of this chapter include (a) our new dynamical extension that identifies unknown curvatures, (b) our proof of global asymptotic stability of the augmented tracking

and curvature identification error dynamics, which is based on a new strict Lyapunov function construction for the augmented error dynamics that gives tracking under constant curvatures, and (c) our robust forward invariance approach to ensuring that the adaptively controlled dynamics respect certain state constraints. The analysis from previous tracking and parameter identification works such as [28] does not apply under unknown curvatures, because of the nonlinear dependence of the dynamics on the curvature. This makes this chapter a significant development that is beyond the scope of [25], [28], and [31]. While [1] and [12] cover more complex dynamics (e.g., for ships, without identifying unknown model parameters), we believe that by covering unknown curvatures and proving robust forward invariance, this chapter is a valuable theoretical step with the potential for more marine robotic applications, where the boundary curves of interest may be uncertain. In Sections 2.2-2.4, we review the necessary background material from [28] and [51], and then we present our new results in the rest of this chapter.

2.2 Deriving the Model

In this section, we derive the basic 2D curve tracking model from [51], which will serve as the basis for the various systems we will study in this chapter. We consider a vehicle moving at constant speed in the plane in the presence of an obstacle. The problem we wish to consider is boundary following with collision avoidance. We represent the obstacle as a simple closed curve in the plane and the vehicle is represented as a point-particle whose motion traces out another curve in the plane. From the viewpoint of mechanics, we are considering particle motion subject to gyroscopic forces, that is, forces which change the direction of motion without changing the kinetic energy and thus speed. The ultimate goal is to design a steering control for our autonomous vehicle, so we derive the model with this in mind.

Consider a point moving at unit speed in the plane in the presence of a single obstacle, i.e. a region of the plane bounded by a simple closed curve. We will assume that this boundary curve is C^2 and that at any given time, the point on the obstacle boundary which is closest to the vehicle is unique. We will refer to this "closest point" on the curve as the *shadow point*. For the sake of deriving the model, we assume that the curvature κ_1 is constant and that $\kappa_1 \geq 0$, that is, our curves represent the boundary of a circle or is a line (but see Section 2.8 for an extension to nonconstant curvatures). Let $\mathbf{r_1}$ denote the position of the shadow point, let $\mathbf{x_1}$ denote the unit tangent vector at the shadow point, and let $\mathbf{y_1}$ denote the unit normal. We will always choose $\mathbf{y_1}$ such that it forms a right-handed frame with $\mathbf{x_1}$; see Figure 2.1. The motion of the shadow point is given by

$$\begin{aligned} \mathbf{r_1'} &= \mathbf{x_1} & \dot{\mathbf{r}}_\mathbf{1} &= v_1\mathbf{x_1} \\ \mathbf{x_1'} &= \kappa_1\mathbf{y_1} & \dot{\mathbf{x}}_\mathbf{1} &= v_1\kappa_1\mathbf{y_1} \\ \mathbf{y_1'} &= -\kappa_1\mathbf{x_1} & \dot{\mathbf{y}}_\mathbf{1} &= -v_1\kappa_1\mathbf{x_1} \end{aligned} \tag{2.1}$$

where $v_1 = ds/dt$. The left and right sets of equations in (2.1) represent differentiation with respect to arc-length and the time variable t respectively.

Similarly, we can derive a set of equations for the motion of our vehicle, where we use the subscript 2 to denote the point representing the vehicle:

$$\begin{aligned} \dot{\mathbf{r}}_\mathbf{1} &= v_1\mathbf{x_1} & \dot{\mathbf{r}}_\mathbf{2} &= \mathbf{x_2} \\ \dot{\mathbf{x}}_\mathbf{1} &= v_1\kappa_1\mathbf{y_1} & \dot{\mathbf{x}}_\mathbf{2} &= u_2\mathbf{y_2} \\ \dot{\mathbf{y}}_\mathbf{1} &= -v_1\kappa_1\mathbf{x_1} & \dot{\mathbf{y}}_\mathbf{2} &= -u_2\mathbf{x_2} \end{aligned} \tag{2.2}$$

where there is no v_2 term because of our unit speed assumption on the vehicle. Recall that steering a vehicle entails changing the curvature of a vehicle's path at its current position. Hence, the curvature κ_2 is denoted by u_2, which is a placeholder for the steering control which will be specified later. We study the coupled dynamics

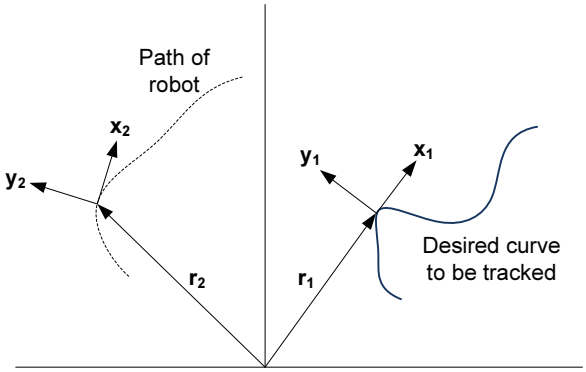

Figure 2.1. Positions and frames for the vehicle $(\mathbf{r_2}, \mathbf{x_2}, \mathbf{y_2})$ and shadow point $(\mathbf{r_1}, \mathbf{x_1}, \mathbf{y_1})$

of our vehicle/shadow point pair. Let $\mathbf{r} = \mathbf{r_2} - \mathbf{r_1}$ be the vector pointing from the shadow point on the curve to the current position of the vehicle. We assume that

$$\mathbf{r} \cdot \mathbf{y_2} \neq 0,$$

holds initially, i.e. our vehicle does not start on the boundary of the obstacle and that the vehicle is not moving directly towards or away from the curve. We will show later that our choice of steering controller ensures that this holds for all future time. We orient the boundary curve such that

$$\mathbf{x_1} \cdot \mathbf{x_2} > \mathbf{0}$$

meaning both the tangent at the shadow point and the heading direction of the vehicle are in the same direction. Our curve forms a region in the plane, so we will assume that our vehicle lies in the exterior region, since in practice our "obstacle" frequently represents a region to be avoided. See Figure 2.1.

Let $\rho = |\mathbf{r}|$ represent the relative separation between these two particles. From basic vector calculus we have

$$\dot{\rho} = \frac{d}{dt}\left(\sqrt{\mathbf{r} \cdot \mathbf{r}}\right) = \frac{1}{2}\left(\frac{\mathbf{r} \cdot \dot{\mathbf{r}} + \dot{\mathbf{r}} \cdot \mathbf{r}}{\sqrt{\mathbf{r} \cdot \mathbf{r}}}\right) = \frac{\mathbf{r} \cdot \dot{\mathbf{r}}}{|\mathbf{r}|}.$$

Applying the dynamics in (2.2) gives us:

$$\frac{\mathbf{r} \cdot \dot{\mathbf{r}}}{|\mathbf{r}|} = \frac{\mathbf{r}}{|\mathbf{r}|} \cdot (\mathbf{x_2} - v_1 \mathbf{x_1}) = \left(\frac{\mathbf{r}}{|\mathbf{r}|} \cdot \mathbf{x_2}\right) - v_1 \left(\frac{\mathbf{r}}{|\mathbf{r}|} \cdot \mathbf{x_1}\right).$$

By definition, the shadow point is the closest point on the curve to the current position of the vehicle. As such, it is an extrema of the function relating the Euclidean distance of the vehicle with any other point on the curve. As a necessary condition for $\mathbf{r_2}$ to be a shadow point, it must satisfy the following identity:

$$\mathbf{r} \cdot \mathbf{x_1} = \mathbf{0} \text{ and equivalently } \mathbf{y_1} = \pm \frac{\mathbf{r}}{|\mathbf{r}|}. \tag{2.3}$$

The first equation implies the tangent to the curve is perpendicular to the vector pointing from the shadow point to the vehicle, and since $\{\mathbf{x_1}, \mathbf{y_1}\}$ form a basis of $\mathbb{R}^2$, the second equation follows from the first and vice versa.

Since our vehicle lies in the exterior of the obstacle, the positive sign corresponds to the case of clockwise motion around the obstacle and the negative sign corresponds to counter-clockwise motion around the obstacle. From the above, we have

$$\dot{\rho} = \pm \mathbf{y_1} \cdot \mathbf{x_2} = \mp \mathbf{x_1} \cdot \mathbf{y_2}, \tag{2.4}$$

for clockwise and counterclockwise motion respectively. Next, we derive an equation for v_1, the speed of the shadow point moving along the boundary curve, using

$$\begin{aligned} \frac{d}{dt}(\mathbf{r} \cdot \mathbf{x_1}) &= \dot{\mathbf{r}} \cdot \mathbf{x_1} + \mathbf{r} \cdot \dot{\mathbf{x}}_\mathbf{1} \\ &= (\mathbf{x_2} - v_1 \mathbf{x_1}) \cdot \mathbf{x_1} + \left(\frac{\mathbf{r} \cdot \mathbf{y_1}}{|\mathbf{r}|} \right) |\mathbf{r}| v_1 \kappa_1 \\ &= \mathbf{x_1} \cdot \mathbf{x_2} - v_1 \pm |\mathbf{r}| v_1 \kappa_1, \end{aligned} \tag{2.5}$$

where the last equality used (2.3). Since $\mathbf{r} \cdot \mathbf{x_1} = \mathbf{0}$, it follows that

$$\mathbf{x_1} \cdot \mathbf{x_2} = v_1 (1 \mp |\mathbf{r}| \kappa_1), \tag{2.6}$$

and thus

$$v_1 = \frac{\mathbf{x_1} \cdot \mathbf{x_2}}{1 \pm \kappa_1 |\mathbf{r}|}.$$

In the case where

$$\left(\tfrac{\mathbf{r}}{|\mathbf{r}|} \cdot \mathbf{y_1} \right) \kappa_1 < 0, \tag{2.7}$$

we say that the boundary curves away from the moving vehicle, and this corresponds to a positive sign in (2.6). Likewise,

$$\left(\frac{\mathbf{r}}{|\mathbf{r}|} \cdot \mathbf{y_1}\right) \kappa_1 > 0 \tag{2.8}$$

corresponds to the boundary curving towards the moving vehicle and a negative sign. We note that there is a singularity in the case of $|\mathbf{r}| = -1/\kappa_1$, which corresponds to the case of lying in the center of the circle (or osculating circle in the case of non-constant curvatures).

2.3 Transforming to Shape Variables

Recall that the goal is to construct a steering controller that ensures curve tracking, namely that our vehicle can move parallel to the boundary curve at some given safe distance. To this end, we use the shape variables $\{\rho, \phi\}$ which represent the relative positions and orientations of the vehicle and the shadow point respectively. Recall from earlier that we defined $\rho = |\mathbf{r}|$ to be the relative distance between the vehicle and the shadow point on the curve. In our analysis, we will choose a constant ρ_0 to be the desired relative distance. Later our control will ensure that $\lim_{t\to+\infty} \rho(t) = \rho_0$ for all initial conditions $\rho(0)$. We let ϕ denote the angle between the heading direction of the vehicle and the tangent vector to the boundary curve at the shadow point such that

$$\mathbf{x_1} \cdot \mathbf{x_2} = \cos\phi. \tag{2.9}$$

Recall that our vehicle is not initially moving directly towards or away from the boundary curve, we will show later that it holds for all $t > 0$ as well. Hence, the ϕ variable satisfies

$$-\frac{\pi}{2} < \phi < \frac{\pi}{2}.$$

We next derive the dynamics of the system in terms of our shape variables.

From (2.4), we choose

$$\dot{\rho} = -\mathbf{x_1} \cdot \mathbf{y_2} = -\sin\phi.$$

Computing the time derivative of $\mathbf{x_1} \cdot \mathbf{y_2}$ and substituting (2.6) and (2.9) gives us

$$\begin{aligned}
\frac{d}{dt}(\mathbf{x_1} \cdot \mathbf{y_2}) &= \dot{\mathbf{x}}_\mathbf{1} \cdot \mathbf{y_2} + \mathbf{x_1} \cdot \dot{\mathbf{y}}_\mathbf{2} \\
&= (v_1\kappa_1(\mathbf{y_1} \cdot \mathbf{y_2}) - u_2(\mathbf{x_1} \cdot \mathbf{x_2}) \\
&= (v_1\kappa_1 - u_2)(\mathbf{x_1} \cdot \mathbf{x_2}) \\
&= \left[\left(\frac{\mathbf{x_1} \cdot \mathbf{x_2}}{1 \pm \kappa_1|\mathbf{r}|}\right)\kappa_1 - u_2\right](\mathbf{x_1} \cdot \mathbf{x_2}) \\
&= \left[\left(\frac{\kappa_1 \cos\phi}{1 \pm \kappa_1|\mathbf{r}|}\right) - u_2\right]\cos\phi
\end{aligned} \tag{2.10}$$

Alternatively,

$$\frac{d}{dt}(\mathbf{x_1} \cdot \mathbf{y_2}) = \frac{d}{dt}(\sin\phi) = (\cos\phi)\dot{\phi}. \tag{2.11}$$

By setting (2.10) equal to (2.11) we obtain

$$\dot{\phi} = \frac{\kappa_1 \cos\phi}{1 \pm \kappa_1|\mathbf{r}|} - u_2. \tag{2.12}$$

Recall that we will assume that our vehicle is exterior to the region bounded by the obstacle. In the case of constant curvatures, this means that our boundary curve will always "curve away" from the vehicle. Hence, we can write the basic curve tracking dynamics with a time-varying uncertainty Δ as

$$\dot{\rho} = -\sin(\phi), \qquad \dot{\phi} = \frac{\kappa\cos(\phi)}{1 + \kappa\rho} - u_2 + \Delta \tag{2.13}$$

where ρ is the distance between the robot and the closest point on the curve being tracked (which we assume is unique), ϕ is the bearing, κ is the curvature at the closest point on the curve, and u_2 is the steering control. Here, Δ is a real-valued essentially bounded function that represents (control, measurement, or model) uncertainty. The state space is $\mathcal{X} = (0, +\infty) \times (-\pi/2, \pi/2)$, i.e., the shape variables (ρ, ϕ) take their values in $\mathcal{X}$.

2.4 Review of Nonadaptive Cases

In the preceding subsection, we showed how the curve tracking dynamics can be simplified to the model (2.13) from [51], having the state space is $\mathcal{X} = (0, +\infty) \times (-\pi/2, \pi/2)$, i.e., (ρ, ϕ) takes its values in $\mathcal{X}$. For the rest of this chapter, we assume that Δ is piecewise continuous. For cases where $\Delta = 0$, the work [51] also designed a feedback to achieve asymptotic stabilization of an equilibrium corresponding to a constant distance ($\rho = \rho_0 > 0$) and zero bearing ($\phi = 0$), which occurs when the robot moves parallel to the curve. Since κ in [25] was assumed to be known, it used the control

$$u_0 = \frac{\kappa \cos(\phi)}{1 + \kappa\rho} - h'(\rho)\cos(\phi) + \mu \sin(\phi) \tag{2.14}$$

where $\mu > 0$ is a steering constant, under this assumption, where $\mathcal{K}_\infty$ is the class of functions that we defined in the previous chapter:

Assumption 1. The function $h : (0, +\infty) \to [0, +\infty)$ is C^2, there are only finitely many' values ρ where $h'(\rho) = 0$, $\lim_{\rho \to 0^+} h(\rho) = \lim_{\rho \to +\infty} h(\rho) = +\infty$, and there is a constant $\rho_0 > 0$ such that $h(\rho_0) = 0$. Also, there exist an increasing C^1 function $\gamma : [0, +\infty) \to [\mu, +\infty)$ and a function $\Gamma \in \mathcal{K}_\infty \cap C^1$ such that $\gamma(h(\rho)) \geq 1 + 0.5\mu^2 + h''(\rho)$ and $\Gamma(h(\rho)) \geq (h'(\rho))^2$ hold for all $\rho > 0$. Finally, $h'(\rho)(\rho - \rho_0)$ is positive for all $\rho > 0$ except for $\rho = \rho_0$, and $h''(\rho_0) > 0$. □

Then, for any constant $L > 0$, [25] shows that the unperturbed closed loop dynamics

$$\dot{\rho} \;=\; -\sin(\phi), \quad \dot{\phi} \;=\; h'(\rho)\cos(\phi) - \mu \sin(\phi), \tag{2.15}$$

admits the strict Lyapunov function

$$\begin{aligned} U(\rho, \phi) \;\; = \;\; & -h'(\rho)\sin(\phi) + \frac{1}{\mu}\int_0^{V(\rho,\phi)} \gamma(m)\mathrm{d}m \\ & + L\Gamma(V(\rho, \phi)) + \frac{1}{2L}V(\rho, \phi) \end{aligned} \tag{2.16}$$

with respect to $((\rho_0, 0), \mathcal{X})$, where

$$V(\rho, \phi) = -\ln\big(\cos(\phi)\big) + h(\rho). \tag{2.17}$$

The function (2.17) was used in [51] to prove global asymptotic stability of (2.15) to $(\rho_0, 0)$, using LaSalle invariance and the fact that

$$\frac{d}{dt}V(\rho(t), \phi(t)) = -\mu \sin^2(\phi)/\cos(\phi) \tag{2.18}$$

holds along all solutions of (2.15) in $\mathcal{X}$.

A key advantage of [25] is that it proves that along all trajectories of (2.15) in $\mathcal{X}$, the function (2.16) satisfies $U \geq V$ and the strict Lyapunov decay condition

$$\dot{U} \;\leq\; -0.5[h'(\rho)\cos(\phi)]^2 - \mathcal{G}(V(\rho, \phi))\sin^2(\phi) \tag{2.19}$$

where $\mathcal{G}(r) = 1+\mu(L\Gamma'(r)+1/(2L))$. The strict Lyapunov function decay condition (2.19) allowed us to prove ISS of

$$\dot{\rho} = -\sin(\phi),\ \dot{\phi} = h'(\rho)\cos(\phi) - \mu\sin(\phi) + \Delta, \tag{2.20}$$

under certain restrictions on the norm $|\Delta|_\infty$ of the perturbation Δ, when κ is a known positive constant.

We also need the following robust forward invariant results from [25]. For any constants $\rho_* \in (0, \rho_0/2)$ and $K > 1$, let $\mu \in (0, \pi/(2\rho_*))$ be a constant such that

$$\mu\tan(\mu\rho_*) > \max\big\{|h'(\rho)| : \rho_* \leq \rho \leq \rho_* + K\rho_0\big\} \tag{2.21}$$

and $H(\rho_*, \mu, K)$ be the closed region in the (ρ, ϕ)-plane that is bounded by the hexagon that has the vertices $A = (\rho_*, 0)^\top$, $B = (2\rho_*, \mu\rho_*)^\top$, $C = (\rho_* + K\rho_0, \mu\rho_*)^\top$, $D = (\rho_* + K\rho_0, 0)^\top$, $E = (K\rho_0, -\mu\rho_*)^\top$, and $F = (\rho_*, -\mu\rho_*)^\top$. Notice that for any compact region $\mathcal{D} \subseteq (0, +\infty) \times (-\pi/2, \pi/2)$, it is possible to choose the parameters in the formulas for the vertices of the hexagon so that the resulting hexagon

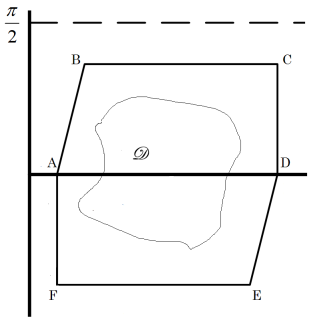

Figure 2.2. Hexagon $H(\rho_*, \mu, K)$

contains $\mathcal{D}$ in its interior. Therefore, while solutions of the system (2.20) having initial states in $\mathcal{D}$ may reach points outside $\mathcal{D}$ in finite time, our restrictions on Δ will ensure that the solutions will remain in $H(\rho_*, \mu, K)$ at all positive times, which is a way to ensure useful tolerance and safety bounds. We represent this useful future using the region inside in the hexagon in Figure 2.2 with a curved boundary.

Set $\Delta_* = \min\{|h'(\rho)\cos(\phi)| : (\rho, \phi)^\top \in \text{AB}\cup\text{ED}\}$ and $\Delta_{**} = \min\{|h'(\rho)\cos(\phi) - \mu\sin(\phi)| : (\rho, \phi)^\top \in \text{BC}\cup\text{EF}\}$. Then $\min\{\Delta_*, \Delta_{**}\} > 0$, by (2.21) and Assumption 1 (using the fact that the first components of B and E are below and above ρ_0, respectively), and [25] and [28] prove the following in terms of U from (2.16), where ∂ will be used to denote a boundary:

Lemma 2.4.1. *Let Assumption 1 hold, $\rho_* \in (0, \rho_0/2)$ and $K > 1$ and $L > 0$ be any constants, and $\mu \in (0, \pi/(2\rho_*))$ satisfy (2.21). Then: (a) For any constant*

$$\bar{\Delta} \in (0, \min\{\Delta_*, \Delta_{**}\}), \tag{2.22}$$

the set $H(\rho_*, \mu, K)$ is robustly forwardly invariant for (2.20) with disturbances valued in $\mathcal{U} = [-\bar{\Delta}, \bar{\Delta}]$. (b) For each constant $\Delta_a > \min\{\Delta_*, \Delta_{**}\}$, we can find a boundary point $\tilde{p} \in \partial(H(\rho_*, \mu, K))$ such that the solution of (2.20) starting at $\tilde{p}$ for one of the constant perturbations $\Delta = \pm\Delta_a$ exits $H(\rho_*, \mu, K)$. (c) There is a constant $v_0 > 0$ such that $U(\rho, \phi) \geq v_0|(\rho - \rho_0, \phi)|^2$ for all $(\rho, \phi) \in H(\rho_*, \mu, K)$. □

Part (b) of Lemma 2.4.1 implies that if we use the control (2.14), then the bound $\min\{\Delta_*, \Delta_{**}\}$ cannot be enlarged without violating the forward invariance requirement, so the bound is optimal and not conservative (but see Section 2.7 for larger perturbation bounds under other controls). Finally, we use the following, whose proof consists of Step 3 of [28, Appendix B]: :

Lemma 2.4.2. *Let $\mathcal{X}^\sharp$ be a bounded robustly forwardly invariant set for (1.3) with disturbances $\delta : [0, +\infty) \to [-\delta_*, \delta_*]$ that are bounded by some constant $\delta_* > 0$ with $\mathcal{F}$ not depending on t, where $\mathcal{F}(0, 0) = 0$. Let $V^\sharp : \mathcal{O} \to [0, +\infty)$ be C^1 on some open set $\mathcal{O}$ containing $\mathcal{X}^\sharp$ and admit a constant $\underline{v} > 0$, a continuous positive definite function $\alpha_0 : [0, +\infty) \to [0, +\infty)$, a function $\bar{\gamma} \in \mathcal{K}_\infty$, and a modulus Λ with respect to $(0, \mathcal{X}^\sharp)$ such that*

$$\frac{d}{dt}V^\sharp \leq -\alpha_0(V^\sharp) + \bar{\gamma}(|\delta|) \tag{2.23}$$

and

$$\underline{v}|x|^2 \leq V^\sharp(x) \leq \Lambda(x) \tag{2.24}$$

hold along all trajectories of (1.3) starting in $\mathcal{X}^\sharp$ for all $\delta : [0, +\infty) \to [-\delta_*, \delta_*]$. Then, we can construct functions $\beta^\sharp \in \mathcal{KL}$ and $\gamma^\sharp \in \mathcal{K}_\infty$ such that

$$|x(t)| \leq \beta^\sharp(\Lambda(x(0)), t) + \gamma^\sharp(|\delta|_{[0,t]}) \tag{2.25}$$

holds along all trajectories of (1.3) starting in $\mathcal{X}^\sharp$ for all choices of δ, so (1.3) is ISS with respect to $([-\delta_*, \delta_*], 0, \mathcal{X}^\sharp)$. □

Condition (2.23) differs from the usual ISS Lyapunov decay condition because α_0 is not required to be of class $\mathcal{K}_\infty$. However, one can prove Lemma 2.4.2 by using the boundedness and robust forward invariance properties of $\mathcal{X}^\sharp$ to convert (2.23) into an ISS Lyapunov function decay condition, by replacing α_0 by a $\mathcal{K}_\infty$ function.

2.5 Main Adaptive Control and Tracking Result

In the next three subsections, we state our main adaptive tracking and parameter identification theorem of this chapter, we provide a key lemma needed for its proof, and then we prove the theorem.

2.5.1 Statement of Result

We leverage the results from the preceding section, to study the two dimensional curve tracking dynamics

$$\dot{\rho} = -\sin\phi, \quad \dot{\phi} = \frac{\kappa\cos\phi}{1+\kappa\rho} - u_2 + \delta \tag{2.26}$$

with unknown constant curvatures κ and piecewise continuous unknown disturbances $\delta : [0, +\infty) \to [-\bar{\delta}, \bar{\delta}]$ with a known bound $\bar{\delta} \geq 0$ (but see Section 2.6 for nonconstant curvatures). The control u_2 in (2.26) will differ from (2.14), since we will no longer assume that κ is known. By writing

$$\frac{\kappa}{1+\kappa\rho} = \frac{\dfrac{\kappa}{1+\kappa\rho_0}}{1+\dfrac{\kappa}{1+\kappa\rho_0}(\rho-\rho_0)} = \frac{\kappa_0}{1+\kappa_0(\rho-\rho_0)} \tag{2.27}$$

where $\rho_0 > 0$ is our desired distance to the curve and

$$\kappa_0 = \frac{\kappa}{1+\kappa\rho_0}, \tag{2.28}$$

we will rescale κ to replace $\kappa/(1+\kappa\rho)$ by $\kappa_0/(1+\kappa_0(\rho-\rho_0))$ in (2.26) and so also in what follows; see Section 2.6 for motivation for the transformation (2.27). Later we specify our robustly forwardly invariant sets to ensure that $1+\kappa_0(\rho-\rho_0)$ stays positive in our domain of interest.

While κ_0 is unknown, we assume that we know constants $\underline{c}$ and $\bar{c}$ such that $\kappa_0 \in (\underline{c}, \bar{c})$. We also assume that Assumption 1 holds. In terms of U from (2.16), we use the estimator

$$\dot{\hat{\kappa}}_0 = (\hat{\kappa}_0 - \underline{c})(\bar{c} - \hat{\kappa}_0)\frac{\cos(\phi)}{(1+(\rho-\rho_0)\hat{\kappa}_0)^2}\frac{\partial U}{\partial\phi}(\rho,\phi) \tag{2.29}$$

for the unknown scaled curvature κ_0. This is valid, because our U in (2.16) does not depend on κ, and because later, we specify our robustly forwardly invariant sets in such a way that $1 + (\rho - \rho_0)\hat{\kappa}_0$ also stays positive. We use

$$u_2 = \frac{\hat{\kappa}_0 \cos(\phi)}{1 + \hat{\kappa}_0(\rho - \rho_0)} - h'(\rho)\cos(\phi) + \mu \sin(\phi) \tag{2.30}$$

where h satisfies Assumption 1. This is valid, because in practice, the current bearing $\phi(t)$ can be detected by sensors, but the curvature κ (which is $\mathrm{d}\phi/\mathrm{d}s$ in terms of the curve length parameter s) is difficult to measure accurately.

Applying (2.27) to (2.26) and taking a common denominator, we conclude that the closed loop dynamics for the augmented error $(\tilde{q}, \tilde{\kappa}_0) = (\tilde{q}_1, \tilde{q}_2, \tilde{\kappa}_0) = (\rho - \rho_0, \phi, \hat{\kappa}_0 - \kappa_0)$ are

$$\begin{cases} \dot{\tilde{q}}_1 &= -\sin(\tilde{q}_2) \\ \dot{\tilde{q}}_2 &= h'(\tilde{q}_1 + \rho_0)\cos(\tilde{q}_2) - \mu \sin(\tilde{q}_2) \\ &\quad - \dfrac{\tilde{\kappa}_0 \cos(\phi)}{(1 + \kappa_0(\rho - \rho_0))(1 + (\kappa_0 + \tilde{\kappa}_0)(\rho - \rho_0))} + \delta \\ \dot{\tilde{\kappa}}_0 &= \dfrac{(\kappa_0 + \tilde{\kappa}_0 - \underline{c})(\bar{c} - \kappa_0 - \tilde{\kappa}_0)}{(1 + (\rho - \rho_0)\hat{\kappa}_0)^2} \cos(\tilde{q}_2) \dfrac{\partial U}{\partial \phi}(\rho, \phi). \end{cases} \tag{2.31}$$

Fix any one of the robustly forwardly invariant hexagons $\mathcal{S} = H(\rho_*, \mu, K)$ from Section 2.4, and any constant such that $\bar{\Delta} \in (0, \min\{\Delta_*, \Delta_{**}\})$, where $\min\{\Delta_*, \Delta_{**}\}$ is from Lemma 2.4.1. Choosing any functions γ and Γ that satisfy Assumption 1 and any constant $L > 0$, and defining V by (2.17), we fix any positive constants $\bar{\mathcal{M}}_1$ and $\bar{\mathcal{M}}_2$ such that

$$\begin{aligned} \bar{\mathcal{M}}_1 &\geq \frac{1}{\mu}\gamma(V(\rho, \phi)) + L\Gamma'(V(\rho, \phi)) + \frac{1}{2L} \quad \text{and} \\ \bar{\mathcal{M}}_2 &\geq \frac{\rho - \rho_0}{h'(\rho)} \max\left\{1, \frac{\rho - \rho_0}{h'(\rho)\cos^2(\phi)}\right\} \end{aligned} \tag{2.32}$$

hold for all $(\rho, \phi) \in \mathcal{S}$ such that $\rho \neq \rho_0$. The constants $\bar{\mathcal{M}}_1$ and $\bar{\mathcal{M}}_2$ exist by the continuity of V on the compact set $\mathcal{S}$, continuity of γ and Γ', and the facts that

$\mu\rho_* < \pi/2$ (which implies that $\cos^2(\phi) \geq \cos^2(\mu\rho_*) > 0$ for all ϕ for which there is a pair $(\rho, \phi) \in \mathcal{S}$) and $h''(\rho_0) > 0$, using L'Hopital's Rule to bound $(\rho - \rho_0)/h'(\rho)$. Our first adaptive control theorem is as follows (where ISS must be understood as a robustness property of (2.31) whose input is the disturbance δ):

Theorem 2.5.1. *Let $\mathcal{S}$, $\bar{\Delta}$, $\bar{\delta} \in [0, \bar{\Delta})$, ρ_0, h, U, $\bar{\mathcal{M}}_1 > 0$, and $\bar{\mathcal{M}}_2 > 0$ satisfy the above requirements, let $\lambda \in (0, 1)$ be any constant, and let the constant bounds for $\underline{c}$ and $\bar{c} > \underline{c}$ for κ_0 satisfy*

$$\bar{c} < \underline{c} + \min\left\{\lambda^2(\bar{\Delta} - \bar{\delta}), \sqrt{\frac{2\lambda^3}{\bar{\mathcal{M}}_1}}, \sqrt{\frac{\lambda^3}{\bar{\mathcal{M}}_2(2 + \bar{\mathcal{M}}_1)}}\right\}, \tag{2.33}$$

$$\bar{c} < \frac{1 - \lambda}{\rho_0 - \rho_*}, \text{ and } \underline{c} > \frac{\lambda - 1}{\rho_* + (K - 1)\rho_0}. \tag{2.34}$$

Then, (2.31) is ISS with respect to $([-\bar{\delta}, \bar{\delta}], 0, \mathcal{S}^\sharp)$ where $\mathcal{S}^\sharp = \{(\tilde{q}, \tilde{\kappa}_0) : \tilde{q} + (\rho_0, 0) \in \mathcal{S}, \tilde{\kappa}_0 + \kappa_0 \in (\underline{c}, \bar{c})\}$. □

The condition $\hat{\kappa}_0 = \tilde{\kappa}_0 + \kappa_0 \in (\underline{c}, \bar{c})$ in the definition of $\mathcal{S}^\sharp$ is the requirement that the estimate $\hat{\kappa}_0$ of κ_0 stays in the interval $(\underline{c}, \bar{c})$ that is known to contain κ_0, which will be guaranteed by the barrier terms $(\kappa_0 + \tilde{\kappa}_0 - \underline{c})(\bar{c} - \kappa_0 - \tilde{\kappa}_0)$ in (2.31). See also Section 2.7 for a method for eliminating the requirement (2.33), based on scaling h and μ in the control.

2.5.2 Key Robust Forward Invariance Lemma

To prove Theorem 2.5.1, we first prove:

Lemma 2.5.1. *Let the assumptions of Theorem 2.5.1 hold. Then for each initial state $(\tilde{q}(0)\tilde{\kappa}_0(0)) \in \mathcal{S}^\sharp$ for (2.31) and each choice of the uncertainty $\delta : [0, +\infty) \to [-\bar{\delta}, \bar{\delta}]$, the solution $(\tilde{q}(t), \tilde{\kappa}_0(t)) = (\rho(t) - \rho_0, \phi(t), \hat{\kappa}_0(t) - \kappa_0)$ for (2.31) satisfies*

$$\min\{1 + \kappa_0\tilde{q}_1(t), 1 + (\kappa_0 + \tilde{\kappa}_0(t))\tilde{q}_1(t)\} \geq \lambda \tag{2.35}$$

for all $t \geq 0$ and $(\tilde{q}(t), \tilde{\kappa}(t)) \in \mathcal{S}^\sharp$ for all $t \geq 0$, so $(\rho(t), \phi(t))$ stays in $\mathcal{S}$. □

Proof: Fix any rectangle $[\rho_{\min}, \rho_{\max}] \times [\phi_{\min}, \phi_{\max}] \subseteq (0, +\infty) \times (-\pi/2, \pi/2)$ such that $\mathcal{S} \subseteq (\rho_{\min}, \rho_{\max}) \times (\phi_{\min}, \phi_{\max})$ and such that

$$\bar{c} < \frac{1-\lambda}{\rho_0 - \rho_{\min}} \text{ and } \underline{c} > \frac{\lambda - 1}{\rho_{\max} - \rho_0} \tag{2.36}$$

hold. This can be done by choosing $\rho_{\min} < \rho_*$ close enough to ρ_*, choosing $\rho_{\max}$ close enough to $\rho_* + K\rho_0$, and using the strictness of the inequalities in (2.34). We first prove that for all $\rho \in [\rho_{\min}, \rho_{\max}]$ and all $r \in [\underline{c}, \bar{c}]$, we have

$$1 + r(\rho - \rho_0) \geq \lambda. \tag{2.37}$$

This will give the required lower bounds (2.35), once we show that $(\tilde{q}(t), \tilde{\kappa}(t)) \in \mathcal{S}^\sharp$ for all $t \geq 0$ when $(\tilde{q}(0), \tilde{\kappa}(0)) \in \mathcal{S}^\sharp$.

Consider three cases. Case 1: If r and $\rho - \rho_0$ are both nonpositive or both nonnegative, then $1 + r(\rho - \rho_0) \geq 1 > \lambda$. Case 2: If $r < 0 \leq \rho - \rho_0$, then $\underline{c} < 0$, so (2.36) gives $r(\rho - \rho_0) \geq \underline{c}(\rho - \rho_0) \geq \underline{c}(\rho_{\max} - \rho_0) > \lambda - 1$. Case 3: If $r > 0 \geq \rho - \rho_0$, then (2.36) gives $r(\rho - \rho_0) \geq r(\rho_{\min} - \rho_0) \geq \bar{c}(\rho_{\min} - \rho_0) > \lambda - 1$, since $\rho_{\min} < \rho_0$. Next, fix any initial state $(\tilde{q}(0), \tilde{\kappa}_0(0)) \in \mathcal{S}^\sharp$ and a δ. Then the existence of the unique maximal solution on some interval $[0, t_{\max})$ follows from the local Lipschitzness of the right side of (2.31), and the fact that the denominators in (2.31) are positive at the initial time (by our analysis of the preceding three cases, and the fact that $\mathcal{S} \subseteq (\rho_{\min}, \rho_{\max}) \times (\phi_{\min}, \phi_{\max})$.

Next, note that (2.33) gives $|\tilde{\kappa}_0(t)| \leq \bar{c} - \underline{c} < \lambda^2(\bar{\Delta} - \bar{\delta})$, so (2.37) (applied with $r = \kappa_0$ and then $r = \hat{\kappa}_0$) gives

$$\left| \frac{\tilde{\kappa}_0(t)\cos(\phi(t))}{(1 + \kappa_0(\rho(t) - \rho_0))(1 + (\kappa_0 + \tilde{\kappa}_0(t))(\rho(t) - \rho_0))} + \delta(t) \right| < \bar{\Delta} \tag{2.38}$$

for all t such that $(\rho(t), \phi(t)) \in [\rho_{\min}, \rho_{\max}] \times [\phi_{\min}, \phi_{\max}]$ and $\hat{\kappa}_0(t) \in (\underline{c}, \bar{c})$. Suppose that $(\tilde{q}(t), \tilde{\kappa}_0(t))$ did not remain in $\mathcal{S}^\sharp$, for the sake of obtaining a contradiction. We could then find a maximal time t_* such that $(\tilde{q}(r), \tilde{\kappa}_0(r)) \in \mathcal{S}^\sharp$ for all $r \in [0, t_*]$.

In fact, $(\rho(t_*), \phi(t_*))$ lies in the boundary $\partial\mathcal{S}$ of $\mathcal{S}$, since the structure of the $\tilde{\kappa}_0$ subdynamics in (2.31) and a uniqueness of solutions argument (which is analogous to [28, Footnote 2]) ensure that $\tilde{\kappa}_0(t)$ cannot reach $-\kappa_0+\underline{c}$ or $-\kappa_0+\bar{c}$, so $\hat{\kappa}_0$ stays in $(\underline{c}, \bar{c})$. Since $\mathcal{S} \subseteq (\rho_{\min}, \rho_{\max}) \times (\phi_{\min}, \phi_{\max})$ is compact, we can find a constant $\varepsilon > 0$ such that the function $\psi : [0, \varepsilon] \to \mathbb{R}^3$ defined by $\psi(t) = (\psi_1(t), \psi_2(t), \psi_3(t)) = (\tilde{q}(t_* + t), \tilde{\kappa}_0(t_* + t))$ is such that $(\psi_1(t) + \rho_0, \psi_2(t))$ starts in $\partial\mathcal{S}$, is valued in $[\rho_{\min}, \rho_{\max}] \times [\phi_{\min}, \phi_{\max}]$, and solves (2.20) on $[0, \varepsilon]$ with

$$\Delta(t) = -\frac{\tilde{\kappa}_0(t_* + t)\cos(\psi_2(t))}{(1 + \kappa_0\psi_1(t))\,(1 + (\kappa_0 + \tilde{\kappa}_0(t_* + t))\psi_1(t))} + \delta(t_* + t)$$

which satisfies $\max_{t\in[0,\varepsilon]} |\Delta(t)| < \bar{\Delta}$, by (2.38). Such an ε exists, by continuity of $(\tilde{q}, \tilde{\kappa}_0)$. Our choice of $\bar{\Delta}$ as a perturbation bound for maintaining forward invariance of $\mathcal{S}$ and the fact that $\psi(t)$ starts in $\mathcal{S}^\sharp$ now imply that ψ stays in $\mathcal{S}^\sharp$ on $[0, \varepsilon]$, so $(\tilde{q}, \tilde{\kappa}_0)$ stays in $\mathcal{S}^\sharp$ on $[0, t_* + \varepsilon]$, contradicting the maximality of t_*. This proves Lemma 2.5.1. □

2.5.3 Stability Analysis and Curvature Identification

We complete the proof of Theorem 2.5.1. Using the decay estimate (2.19) over $\mathcal{S}$ and the fact that $\hat{\kappa}_0 = \tilde{\kappa}_0 + \kappa_0$ stays in $(\underline{c}, \bar{c})$, it follows that along all trajectories of (2.31) in its forwardly invariant set $\mathcal{S}^\sharp$, the function

$$U^\sharp(\rho, \phi, \tilde{\kappa}_0) = U(\rho, \phi) + \int_0^{\tilde{\kappa}_0} \frac{\ell}{(\ell + \kappa_0 - \underline{c})(\bar{c} - \ell - \kappa_0)} \mathrm{d}\ell \tag{2.39}$$

satisfies

$$\begin{aligned}
\dot{U}^\sharp \;\leq\; & -\frac{1}{2}\big(h'(\rho)\cos(\phi)\big)^2 - \mathcal{G}(V(\rho,\phi))\sin^2(\phi) \\
& - \frac{\partial U}{\partial \phi}(\rho,\phi)\frac{\tilde{\kappa}_0\cos(\phi)}{(1 + \kappa_0(\rho - \rho_0))(1 + (\kappa_0 + \tilde{\kappa}_0)(\rho - \rho_0))} \\
& + \left(\tilde{\kappa}_0\frac{\cos(\phi)}{(1 + \hat{\kappa}_0(\rho - \rho_0))^2} + \delta\right)\frac{\partial U}{\partial \phi}(\rho,\phi) \\
= \;& -\frac{1}{2}\big(h'(\rho)\cos(\phi)\big)^2 - \mathcal{G}(V(\rho,\phi))\sin^2(\phi) \\
& + \left\{\frac{\partial U}{\partial \phi}(\rho,\phi)\frac{\cos(\phi)(-\tilde{\kappa}_0^2)(\rho - \rho_0)}{(1 + \hat{\kappa}_0(\rho - \rho_0))^2(1 + \kappa_0(\rho - \rho_0))}\right\} + \delta\frac{\partial U}{\partial \phi}(\rho,\phi),
\end{aligned} \tag{2.40}$$

where the denominator terms in (2.39) were used to cancel the barrier terms in (2.31) and are nonzero because of the argument cited previously from [28, Footnote 2]. By (2.32) and the facts that $(\rho(t), \phi(t))$ stays in $\mathcal{S}$ (by Lemma 2.5.1) and $(\partial V/\partial\phi)(\rho,\phi) = \tan(\phi)$ on $\mathcal{S}$, our choice (2.16) of U gives

$$\begin{aligned} \left|\tfrac{\partial U}{\partial \phi}(\rho,\phi)\right| &\leq \Big|-h'(\rho)\cos(\phi) + \Big(\tfrac{1}{\mu}\gamma(V(\rho,\phi)) \\ &\qquad + L\Gamma'(V(\rho,\phi)) + 1/(2L)\Big)\tan(\phi)\Big| \\ &\leq \left|h'(\rho)\cos(\phi)\right| + \bar{\mathcal{M}}_1\left|\tan(\phi)\right| \end{aligned} \tag{2.41}$$

on our robustly forwardly invariant set $\mathcal{S}$.

Hence, we can use (2.35) and the triangle inequality to upperbound the quantity in curly braces in (2.40) by

$$\begin{aligned} &\tfrac{\tilde{\kappa}_0^2}{\lambda^3}\big(|h'(\rho)(\rho-\rho_0)|\cos^2(\phi) + \bar{\mathcal{M}}_1|\sin(\phi)(\rho-\rho_0)|\big) \\ &\leq \tfrac{\tilde{\kappa}_0^2}{\lambda^3}\big(|h'(\rho)(\rho-\rho_0)|\cos^2(\phi) + \frac{\bar{\mathcal{M}}_1}{2}\sin^2(\phi + \frac{\bar{\mathcal{M}}_1}{2}(\rho-\rho_0)^2\big) \\ &\leq \tfrac{\tilde{\kappa}_0^2}{\lambda^3}\Big(\bar{\mathcal{M}}_2\big(h'(\rho)\cos(\phi)\big)^2 + \frac{\bar{\mathcal{M}}_1}{2}\sin^2(\phi) \\ &\quad + \frac{\bar{\mathcal{M}}_1}{2}\bar{\mathcal{M}}_2\big(h'(\rho)\cos(\phi)\big)^2\Big). \end{aligned} \tag{2.42}$$

Also, $|\tilde{\kappa}_0|$ is bounded by $\bar{c} - \underline{c}$, (2.33) implies that

$$\frac{1}{\lambda^3}(\bar{c}-\underline{c})^2\bar{\mathcal{M}}_2\left(1 + \frac{1}{2}\bar{\mathcal{M}}_1\right) < \frac{1}{2} \text{ and } \frac{1}{\lambda^3}(\bar{c}-\underline{c})^2\frac{\bar{\mathcal{M}}_1}{2} < 1, \tag{2.43}$$

and the function $\mathcal{G}(r) = 1 + \mu(L\Gamma'(r) + 1/(2L))$ from Section 2.4 is bounded from below by 1.

Hence, (2.40) and (2.42) give a constant $\beta_0 > 0$ such that

$$\begin{aligned} \dot{U}^\sharp &\leq -\frac{1}{2}(h'(\rho)\cos(\phi))^2 - \sin^2(\phi) \\ &\quad + \frac{1}{\lambda^3}(\bar{c}-\underline{c})^2\left(\bar{\mathcal{M}}_2\left(1 + \frac{\bar{\mathcal{M}}_1}{2}\right)(h'(\rho)\cos(\phi))^2\right. \\ &\quad \left. + \frac{\bar{\mathcal{M}}_1}{2}\sin^2(\phi)\right) + \delta\frac{\partial U}{\partial\phi}(\rho,\phi) \\ &\leq -\beta_0\Big((h'(\rho)\cos(\phi))^2 + \sin^2(\phi)\Big) + \delta\frac{\partial U}{\partial\phi}(\rho,\phi) \end{aligned} \tag{2.44}$$

holds along all trajectories of (2.31) in $\mathcal{S}^\sharp$, namely,

$$\beta_0 = \min\left\{\frac{1}{2} - \frac{(\bar{c}-\underline{c})^2}{\lambda^3}\bar{\mathcal{M}}_2\left(1+\frac{\bar{\mathcal{M}}_1}{2}\right), 1 - \frac{(\bar{c}-\underline{c})^2}{2\lambda^3}\bar{\mathcal{M}}_1\right\}.$$

We next convert $U^\sharp$ into a strict Lyapunov function for (2.31) with respect to the zero equilibrium on the set $S^\sharp$, having the form

$$V^\sharp(\tilde{q},\tilde{\kappa}_0) = \bar{\mathcal{M}}_3 U^\sharp(\rho,\phi,\tilde{\kappa}_0) + \tilde{q}_2\tilde{\kappa}_0 \tag{2.45}$$

for a suitable constant $\bar{\mathcal{M}}_3 > 0$. To this end, we first pick a constant $\bar{\mathcal{G}}_1 > \bar{c} - \underline{c}$ such that

$$\left|\frac{\partial U}{\partial \phi}(\rho,\phi)\right| \le \bar{\mathcal{G}}_1,\ \left|\dot{\tilde{\kappa}}_0\right| \le \bar{\mathcal{G}}_1\left|\tilde{q}\right|,\ \text{ and }\ U^\sharp(\rho,\phi,\tilde{\kappa}_0) \ge \frac{|(\tilde{q},\tilde{\kappa}_0)|^2}{\bar{\mathcal{G}}_1} \tag{2.46}$$

for all $(\tilde{q},\tilde{\kappa}_0) \in \mathcal{S}^\sharp$ for all $t \ge 0$. Such a $\bar{\mathcal{G}}_1$ exists by (2.35), (2.41), part (c) of Lemma 2.4.1, and nonnegativity of the integral in (2.39). Then we can use (2.35), (2.46), the fact that $h'(\rho_0) = 0$, the bounds $|\tilde{\kappa}_0(t)| \le \bar{c} - \underline{c}$ and $\cos(\phi) \ge \cos(\mu\rho_*) > 0$, and the triangle inequality to find constants $\bar{\mathcal{G}}_2 > 0$ and $\bar{\mathcal{G}}_3 > 0$ such that along all solutions of (2.31) on $\mathcal{S}^\sharp$ for all $t \ge 0$, we get

$$\begin{aligned}
\frac{d}{dt}(\tilde{q}_2\tilde{\kappa}_0) &\le \Big(h'(\tilde{q}_1+\rho_0)\cos(\tilde{q}_2) - \mu\sin(\tilde{q}_2) \\
&\qquad - \frac{\tilde{\kappa}_0\cos(\phi)}{(1+\kappa_0(\rho-\rho_0))(1+\hat{\kappa}_0(\rho-\rho_0))}\Big)\tilde{\kappa}_0 \\
&\qquad + \bar{\mathcal{G}}_1\left(|\tilde{q}|^2 + |\delta|\right) \\
&\le \bar{\mathcal{G}}_2\left(|\tilde{\kappa}_0||\tilde{q}| + |\tilde{q}|^2\right) - \bar{\mathcal{G}}_3\tilde{\kappa}_0^2 + \bar{\mathcal{G}}_1|\delta| \\
&\le \bar{\mathcal{G}}_2\left(\frac{\bar{\mathcal{G}}_2}{2\bar{\mathcal{G}}_3}|\tilde{q}|^2 + \frac{\bar{\mathcal{G}}_3}{2\bar{\mathcal{G}}_2}\tilde{\kappa}_0^2 + |\tilde{q}|^2\right) - \bar{\mathcal{G}}_3\tilde{\kappa}_0^2 + \bar{\mathcal{G}}_1|\delta| \\
&= \bar{\mathcal{G}}_2\left(\frac{\bar{\mathcal{G}}_2}{2\bar{\mathcal{G}}_3} + 1\right)|\tilde{q}|^2 - \frac{1}{2}\bar{\mathcal{G}}_3\tilde{\kappa}_0^2 + \bar{\mathcal{G}}_1|\delta|.
\end{aligned} \tag{2.47}$$

We can also find a constant $c_0 > 0$ such that

$$\beta_0\left(\left(h'(\rho)\cos(\phi)\right)^2 + \sin^2(\phi)\right) \ \ge\ c_0|\tilde{q}|^2 \tag{2.48}$$

so $\dot{U}^\sharp \leq -c_0|\tilde{q}|^2 + \bar{\mathcal{G}}_1|\delta|$ on $\mathcal{S}^\sharp$, using (2.44) and L'Hopital's rule, since $h''(\rho_0) > 0$ and $\cos(\phi) \geq \cos(\mu\rho_*) > 0$ on $\mathcal{S}$ and $h'(\rho)(\rho - \rho_0) > 0$ for all $\rho \neq \rho_0$.

Hence, the choice (2.45) of $V^\sharp$, with the constant

$$\bar{\mathcal{M}}_3 = 1 + \bar{\mathcal{G}}_1 + \frac{1}{c_0}\bar{\mathcal{G}}_2\left(\frac{\bar{\mathcal{G}}_2}{2\bar{\mathcal{G}}_3} + 1\right), \tag{2.49}$$

implies that on $\mathcal{S}^\sharp$, we can find a constant $\bar{\mathcal{G}}_4 > 0$ such that

$$\begin{aligned}
\dot{V}^\sharp(\tilde{q}, \tilde{\kappa}_0) &\leq -\bar{\mathcal{M}}_3 c_0|\tilde{q}|^2 + \frac{d}{dt}(\tilde{q}_2\tilde{\kappa}_0) + \bar{\mathcal{G}}_4|\delta| \\
&\leq -c_0|\tilde{q}|^2 - \bar{\mathcal{G}}_2\left(\frac{\bar{\mathcal{G}}_2}{2\bar{\mathcal{G}}_3} + 1\right)|\tilde{q}|^2 + \frac{d}{dt}(\tilde{q}_2\tilde{\kappa}_0) + \bar{\mathcal{G}}_4|\delta| \\
&\leq -\underline{v}|(\tilde{q}, \tilde{\kappa}_0)|^2 + \left(\bar{\mathcal{G}}_1 + \bar{\mathcal{G}}_4\right)|\delta|
\end{aligned}$$

and

$$V^\sharp(\tilde{q}, \tilde{\kappa}_0) \geq \frac{\bar{\mathcal{M}}_3|(\tilde{q}, \tilde{\kappa}_0)|^2}{\bar{\mathcal{G}}_1} - 0.5|\tilde{q}|^2 - 0.5\tilde{\kappa}_0^2 \geq \underline{v}|(\tilde{q}, \tilde{\kappa}_0)|^2, \tag{2.50}$$

where $\underline{v} = \min\{c_0, \bar{\mathcal{G}}_3/2, 1/2\}$, by (2.45)-(2.47).

Also, the following variant of an argument from Appendix B in [28] provides a positive definite function α_0 such that

$$\alpha_0\big(V^\sharp(\tilde{q}, \tilde{\kappa}_0)\big) \leq \underline{v}|(\tilde{q}, \tilde{\kappa}_0)|^2 \text{ for all } (\tilde{q}, \tilde{\kappa}_0) \in \mathcal{S}^\sharp. \tag{2.51}$$

We choose any constant

$$\varepsilon \in (0, 0.5\min\{\bar{c} - \kappa_0, \kappa_0 - \underline{c}\}). \tag{2.52}$$

Then (i) there is a function $\alpha_1 \in \mathcal{K}_\infty$ such that $V^\sharp(\tilde{q}, \tilde{\kappa}_0) \leq \alpha_1(|(\tilde{q}, \tilde{\kappa}_0)|)$ for all $(\tilde{q}, \tilde{\kappa}_0) \in \mathcal{S}^\sharp$ such that $\tilde{\kappa}_0 \in [\underline{c} - \kappa_0 + \varepsilon, \bar{c} - \kappa_0 - \varepsilon]$ and (ii) there is a constant $c_1 > 0$ such that $c_1 \leq \underline{v}|(\tilde{q}, \tilde{\kappa}_0)|^2$ for all other points $(\tilde{q}, \tilde{\kappa}_0) \in \mathcal{S}^\sharp$. Hence, by separately considering the cases (i) and (ii), we conclude that (2.51) holds with

$$\alpha_0(r) = \min\{c_1, \underline{v}[\alpha_1^{-1}(r)]^2\}. \tag{2.53}$$

This gives

$$\dot{V}^\sharp(\tilde{q}, \tilde{\kappa}_0) \leq -\alpha_0(V^\sharp(\tilde{q}, \tilde{\kappa}_0)) + \left(\bar{\mathcal{G}}_1 + \bar{\mathcal{G}}_4\right)|\delta| \tag{2.54}$$

along all trajectories of the (2.31) in $\mathcal{S}^\sharp$. Hence, Theorem 2.5.1 follows from (2.50), (2.54), and Lemma 2.4.2.

2.6 Discussion on Assumptions and Extensions

Theorem 2.5.1 applies when κ_0 in (2.31) lies in $(\underline{c}, \bar{c})$, for any constants $\underline{c} \geq 0$ and $\bar{c} > \underline{c}$ satisfying (2.33)-(2.34). However, our derivation of (2.31) was based on the rescaling (2.27) of the curvature to replace the denominator $1 + \kappa\rho$ in (2.26) by $1 + \kappa_0(\rho - \rho_0)$. The rescaling was used to introduce the $\rho - \rho_0$ terms in (2.42), and was also key to ensuring parameter identification, which would not be possible using standard adaptive techniques (which generally provide tracking of the states but not convergence of the parameter estimate to the true parameter value under state constraints). In terms of the curvature parameter κ from the original model (2.26), our bound requirements are then $\underline{c} < \kappa/(1+\kappa\rho_0) < \bar{c}$, by our relation (2.28) between κ_0 and κ.

In robotics, curve tracking is usually done for straight lines or circles, or curves whose curvatures change slowly relative to the convergence speed of the robot and so can be regarded as constant. This is analogous to drivers of cars, who prefer roads that do not have large curvatures, and this motivated our assumption of constant curvatures. However, we can generalize our results to allow nonconstant curvatures that can take negative values. For instance, assume that the unknown curvature is some function $\kappa^\sharp(s) = \kappa + \eta(s)$ of the curve length s for some constant $\kappa > 0$, and that we know a constant $\bar{\delta} \in (0, \kappa)$ such that $\sup_s |\eta(s)| \leq \bar{\delta}$. Then replacing κ by $\kappa^\sharp(s)$ in (2.26) produces

$$\dot{\rho} = -\sin\phi, \quad \dot{\phi} = \frac{\kappa\cos\phi}{1+\kappa\rho} - u_2 + \delta \tag{2.55}$$

with the unknown constant nominal curvature $\kappa \geq 0$, where

$$\delta = \frac{\cos(\phi)\eta(s)}{(1 + (\kappa + \eta(s))\rho)(1 + \kappa\rho)} \tag{2.56}$$

is bounded by $\bar{\delta}$. Then Theorem 2.5.1 ensures ISS with respect to δ (but see below for another approach under nonconstant κ's, where we can often ensure that $\lim_{t\to+\infty}(\rho(t), \phi(t)) = (\rho_0, 0)$, instead of the weaker ISS property). Also, we can satisfy our requirements using $h(\rho) = \alpha(\rho - \rho_0)^2$ for any constant $\alpha > 0$, by only requiring the conditions from Assumption 1 to hold for all $\rho \in [\rho_*, \rho_* + K\rho_0]$, since this implies that (2.19) holds on $\mathcal{S}$, so the requirement $\lim_{\rho\to 0^+} h(\rho) = +\infty$ is not needed in $\mathcal{S}$.

Here is one way to allow larger scaled curvature bounds $\bar{c}$. The second inequality in (2.43) was used to ensure that the term $-\mathcal{G}(V(\rho, \phi)) \sin^2(\phi)$ in (2.40) had a larger magnitude than $(1/\lambda^3)\tilde{\kappa}_0^2(\bar{\mathcal{M}}_1/2)\sin^2(\phi)$ in (2.42), where $\mathcal{G}$ is defined in Section 2.4. If we make the choices of γ and Γ from [25], then since $\mathcal{G}$ is bounded below by $1 + \mu(L(18\alpha/\rho_0) + 1/(2L))$, it follows that Theorem 2.5.1 remains true if we replace the second inequality in (2.43) by

$$\frac{1}{\lambda^3}(\bar{c} - \underline{c})^2 \frac{\bar{\mathcal{M}}_1}{2} < 1 + \mu\left(\frac{18L\alpha}{\rho_0} + \frac{1}{2L}\right). \tag{2.57}$$

Hence, Theorem 2.5.1 remains true if we replace $\sqrt{2\lambda^3/\bar{\mathcal{M}}_1}$ on the right side of (2.33) by the larger upper bound

$$\sqrt{\frac{2\lambda^3}{\bar{\mathcal{M}}_1}}\left(1 + \mu\left(\frac{18L\alpha}{\rho_0} + \frac{1}{2L}\right)\right)^{1/2}. \tag{2.58}$$

We next give another approach to enlarging the curvature bound. For an application of Theorem 2.5.1, see Section 2.9.

2.7 Effects of Scaling Control Terms

It is natural to surmise that scaling $\mu > 0$ and h in the formula (2.30) for the control by large enough constants (without scaling the curvature term in (2.30))

should make it possible to extend our analysis to allow any curvature values for which the denominator in our adaptive control formula (2.30) is never zero, because it makes the curvature term small relative to the other terms in the control. In this section, we study the effects of such scalings, which allow us to drop the condition (2.33) on $\bar{c}$ and make it possible to obtain ISS under larger perturbation bounds, and which therefore allow larger sup norms on the nonconstant parts $\eta(s)$ of the curvatures from the previous section; see (2.56).

To this end, we replace the control u_0 from (2.14), the nonstrict Lyapunov function V from (2.17), and the strictified Lyapunov function U from (2.16) by their scaled analogs

$$\begin{aligned} u_{s,0} &= \frac{\kappa\cos(\phi)}{1+\kappa\rho} - \mathcal{M}_* h'(\rho)\cos(\phi) + \mathcal{M}_*\mu\sin(\phi), \\ V_s(\rho,\phi) &= -\frac{1}{\mathcal{M}_*}\ln(\cos(\phi)) + h(\rho), \text{ and} \\ U_s(\rho,\phi) &= -\frac{1}{\mathcal{M}_*}h'(\rho)\sin(\phi) + \frac{1}{\mu}\int_0^{V_s(\rho,\phi)}\gamma(m)\mathrm{d}m \\ &\quad + \frac{L}{\mathcal{M}_*}\Gamma(V_s(\rho,\phi)) + \frac{1}{2L}V_s(\rho,\phi), \end{aligned} \tag{2.59}$$

respectively, where the constant $\mathcal{M}_* \geq 1$ will be chosen, and $L > 0$ is a tuning constant as before. We assume that Assumption 1 holds, and that h'' is nonnegative valued. Before explaining how the scaling constant effects the proof of Theorem 2.5.1, we first explain how the preliminary results from Section 2.4 must be changed to account for $\mathcal{M}_*$.

First notice that with the new control $u_{s,0}$, the closed loop nonadaptive unperturbed dynamics (2.15) must become

$$\begin{cases} \dot{\rho} &= -\sin(\phi) \\ \dot{\phi} &= \mathcal{M}_* h'(\rho)\cos(\phi) - \mathcal{M}_*\mu\sin(\phi). \end{cases} \tag{2.60}$$

Also, along all solutions of (2.60) in $(0,+\infty)\times(-\pi/2,\pi/2)$, we still have the nonstrict Lyapunov function decay condition $\dot{V} = -\mu\sin^2(\phi)/\cos(\phi)$, since we

can use the $\mathcal{M}_*$ in the formula for V_s to cancel the $\mathcal{M}_*$'s in (2.20). If we choose $N(\rho,\phi) = -h'(\rho)\sin(\phi)$, then

$$\begin{aligned}\frac{1}{\mathcal{M}_*}\dot{N}(\rho,\phi) &= \frac{1}{\mathcal{M}_*}\left[h''(\rho)\sin^2(\phi)\right.\\ &\quad \left.-h'(\rho)\cos(\phi)\left(\mathcal{M}_* h'(\rho)\cos(\phi) - \mathcal{M}_*\mu\sin(\phi)\right)\right]\\ &\leq h''(\rho)\sin^2(\phi) - \frac{1}{2}(h'(\rho)\cos(\phi))^2 + \frac{1}{2}\mu^2\sin^2(\phi),\end{aligned}$$

holds along all trajectories of (2.60), by the triangle inequality $h'(\rho)\cos(\phi)\mu\sin(\phi) \leq \frac{1}{2}(h'(\rho)\cos(\phi))^2 + \frac{1}{2}\mu^2\sin^2(\phi)$. Hence, the same argument (from the proof of [25, Theorem 1]) that led to (2.19) gives

$$\begin{aligned}&\dot{U}_s \leq -0.5[h'(\rho)\cos(\phi)]^2 - \mathcal{G}_s(V_s(\rho,\phi))\sin^2(\phi)\\ &\text{and } \; U_s(\rho,\phi) \geq V_s(\rho,\phi)\end{aligned} \tag{2.61}$$

along all trajectories of (2.60) in $(0,+\infty)\times(-\pi/2,\pi/2)$, where $\mathcal{G}_s$ is defined by $\mathcal{G}_s(r) = 1 + \mu(L\Gamma'(r)/\mathcal{M}_* + 1/(2L))$.

We also change the top left and bottom right vertices B and E of our hexagons from Section 2.4 to

$$\begin{aligned}B &= \left(\rho_*\left(1+(1/\mathcal{M}_*)\right), \mu\rho_*\right) \text{ and}\\ E &= \left(K\rho_0 + \left(1-(1/\mathcal{M}_*)\right)\rho_*, -\mu\rho_*\right)\end{aligned} \tag{2.62}$$

respectively, and keep all other vertices unchanged. Then the new slope for the legs AB and DE is $\mathcal{M}_*\mu$. This changes the supremum $\bar{\Delta}$ for the allowable perturbation bound from $\bar{\Delta}$ to $\mathcal{M}_*\bar{\Delta}$, by a similar proof to that of [25, Theorem 2], except with the intercept function

$$\mathcal{I}(\rho,\phi) = \phi - \mu\rho \tag{2.63}$$

in the earlier proof replaced by $\mathcal{I}_s(\rho,\phi) = \phi - \mathcal{M}_*\mu\rho$.

With these changes, we now define $\mathcal{S}$, $\bar{\Delta}$, $\bar{\delta} \in (0,\bar{\Delta})$, ρ_0, h, $\bar{\mathcal{M}}_1$, and $\bar{\mathcal{M}}_2$ as before, and the new update law

$$\dot{\hat{\kappa}}_0 = (\hat{\kappa}_0 - \underline{c})(\bar{c} - \hat{\kappa}_0)\frac{\cos(\phi)}{(1+(\rho-\rho_0)\hat{\kappa}_0)^2}\frac{\partial U_s}{\partial\phi}(\rho,\phi). \tag{2.64}$$

We use the preceding estimator $\hat{\kappa}_0$ for the scaled curvature κ_0 in the new control

$$u_2 = \frac{\hat{\kappa}_0 \cos(\phi)}{1 + \hat{\kappa}_0(\rho - \rho_0)} - \mathcal{M}_* h'(\rho)\cos(\phi) + \mathcal{M}_* \mu \sin(\phi), \tag{2.65}$$

which produces the augmented error dynamics

$$\begin{cases} \dot{\tilde{q}}_1 &= -\sin(\tilde{q}_2) \\ \dot{\tilde{q}}_2 &= \mathcal{M}_* h'(\tilde{q}_1 + \rho_0)\cos(\tilde{q}_2) - \mathcal{M}_* \mu \sin(\tilde{q}_2) \\ & \quad - \dfrac{\tilde{\kappa}_0 \cos(\phi)}{(1 + \kappa_0(\rho - \rho_0))(1 + (\kappa_0 + \tilde{\kappa}_0)(\rho - \rho_0))} + \delta \\ \dot{\tilde{\kappa}}_0 &= \dfrac{(\kappa_0 + \tilde{\kappa}_0 - \underline{c})(\bar{c} - \kappa_0 - \tilde{\kappa}_0)}{(1 + (\rho - \rho_0)\hat{\kappa}_0)^2} \cos(\tilde{q}_2) \dfrac{\partial U_s}{\partial \phi}(\rho, \phi). \end{cases} \tag{2.66}$$

for the error variable $(\tilde{q}, \tilde{\kappa}_0) = (\tilde{q}_1, \tilde{q}_2, \tilde{\kappa}_0) = (\rho - \rho_0, \phi, \hat{\kappa}_0 - \kappa_0)$ as before. Then we can prove the following result, which allows us to drop the requirement (2.33) on $\underline{c}$ and $\bar{c}$:

Theorem 2.7.1. *Let $\mathcal{S}$, $\bar{\Delta}$, ρ_0, h, $\bar{\mathcal{M}}_1$, and $\bar{\mathcal{M}}_2$ satisfy the above requirements, let $\lambda \in (0,1)$ be any constant, and let the constants $\mathcal{M}_* \geq 1$, $\bar{\delta} \in [0, \mathcal{M}_* \bar{\Delta})$, $\underline{c}$, and $\bar{c} > \underline{c}$ satisfy*

$$\mathcal{M}_* > \max\{\mathcal{M}_A, \mathcal{M}_B\}, \quad \bar{c} < \frac{1-\lambda}{\rho_0 - \rho_*}, \text{ and } \underline{c} > \frac{\lambda - 1}{\rho_* + (K-1)\rho_0}, \tag{2.67}$$

where

$$\mathcal{M}_A = \frac{1}{\bar{\Delta}} \left(\frac{1-\lambda}{\lambda^2} \left(\frac{1}{\rho_0 - \rho_*} + \frac{1}{\rho_* + (K-1)\rho_0} \right) + \bar{\delta} \right) \tag{2.68}$$

and

$$\mathcal{M}_B = \max\left\{ 0.5\bar{\mathcal{M}}_1, \bar{\mathcal{M}}_2(2 + \bar{\mathcal{M}}_1) \right\} \frac{(1-\lambda)^2}{\lambda^3} \left(\frac{1}{\rho_0 - \rho_*} + \frac{1}{\rho_* + (K-1)\rho_0} \right)^2. \tag{2.69}$$

Then, (2.66) is ISS with respect to $([-\bar{\delta}, \bar{\delta}], 0, \mathcal{S}^\sharp)$ where $\mathcal{S}^\sharp = \{(\tilde{q}, \tilde{\kappa}_0) : \tilde{q} + (\rho_0, 0) \in \mathcal{S}, \tilde{\kappa}_0 + \kappa_0 \in (\underline{c}, \bar{c})\}$. □

Proof: We indicate the changes in the proof of Theorem 2.5.1 that are needed to prove Theorem 2.7.1. We replace V and U in the proof of Theorem 2.5.1 by

their scaled versions from (2.59), and we scale $h'(\tilde{q}_1+\rho_0)\cos(\tilde{q}_2)-\mu\sin(\tilde{q}_2)$ by $\mathcal{M}_*$. Since

$$\frac{\partial V_s(\rho,\phi)}{\partial\phi}=\frac{\tan(\phi)}{\mathcal{M}_*}, \tag{2.70}$$

and since the $-h'(\rho)\sin(\phi)$ in the formula for U was scaled by $1/\mathcal{M}_*$ in the formula for U_s, we can replace (2.41) by

$$\left|\frac{\partial U}{\partial\phi}(\rho,\phi)\right|\le\frac{1}{\mathcal{M}_*}\left(\left|h'(\rho)\cos(\phi)\right|+\bar{\mathcal{M}}_1\left|\tan(\phi)\right|\right). \tag{2.71}$$

This lets us scale the left sides of (2.43) by $1/\mathcal{M}_*$, so since our maximal allowable perturbation bound is now $\mathcal{M}_*\bar{\Delta}$, the proof of Theorem 2.5.1 shows that its conclusions stay true if

$$\bar{c}<\underline{c}+\min\left\{\lambda^2\big(\mathcal{M}_*\bar{\Delta}-\bar{\delta}\big),\sqrt{\frac{2\lambda^3\mathcal{M}_*}{\bar{\mathcal{M}}_1}},\sqrt{\frac{\lambda^3\mathcal{M}_*}{\bar{\mathcal{M}}_2(2+\bar{\mathcal{M}}_1)}}\right\}, \tag{2.72}$$

$$\bar{c}<\frac{1-\lambda}{\rho_0-\rho_*}\quad\text{and}\quad\underline{c}>\frac{\lambda-1}{\rho_*+(K-1)\rho_0} \tag{2.73}$$

are all satisfied. The theorem now follows because our lower bounds for $\mathcal{M}_*$ in (2.67) and for $\underline{c}$ in (2.73) imply that

$$\begin{aligned}&\underline{c}+\min\left\{\lambda^2(\mathcal{M}_*\bar{\Delta}-\bar{\delta}),\sqrt{\frac{2\lambda^3\mathcal{M}_*}{\bar{\mathcal{M}}_1}},\sqrt{\frac{\lambda^3\mathcal{M}_*}{\bar{\mathcal{M}}_2(2+\bar{\mathcal{M}}_1)}}\right\}\\&\ge\frac{1-\lambda}{\rho_0-\rho_*},\end{aligned} \tag{2.74}$$

so we can omit the bound (2.72), since it follows from (2.73). □

Remark 1. Our proof of Theorem 2.7.1 shows that we can omit $1/(\rho_*+(K-1)\rho_0)$ from (2.68)-(2.69) when κ_0 is known to be positive, because in that case, we can choose $\underline{c}=0$. When we can scale the steering constant μ and h in the control, we can sometimes use Theorem 2.7.1 to get larger bounds on $\bar{c}$ than what we would get from Theorem 2.5.1; see Section 2.9. □

In the next section, we provide another variant of Theorem 2.5.1, which uses an artificial neural network approach to prove curve tracking under uncertain nonconstant curvatures.

2.8 Unknown Nonconstant Curvatures

Theorems 2.5.1 and 2.7.1 provide curve tracking and parameter identification under state constraints and control uncertainty. However, Theorems 2.5.1 and 2.7.1 require that the scaled curvatures κ_0 (and so also the curvatures κ in the original dynamics) be constant, and our ISS extension from Section 2.6 provides ISS with respect to nonconstant parts $\eta(s)$ of nonconstant curvatures $\kappa^\sharp(s) = \kappa + \eta(s)$ with constant parts κ, without ensuring the curve tracking condition that $\lim_{t\to+\infty}(\rho(t), \phi(t)) = (\rho_0, 0)$. In this section, we give a partial extension of Theorem 2.5.1 to cases where the scaled curvature κ_0 is again a function of arc length s, and where we have an artificial neural network expansion approximation

$$\kappa_0(s) = \sum_{i=1}^{m} w_i \Phi_i(s), \tag{2.75}$$

where the Φ_i's are known continuous basis functions, the unknown weights w_i are independent of s and lie in known intervals of the form $(\underline{w}_i, \bar{w}_i)$ for $i = 1, 2, \ldots, m$ with constant endpoints, and $m \geq 1$; see [49] for background on artificial neural networks. We again assume that we know constant upper and lower bounds for the curvature, i.e., constants $\bar{c}$ and $\underline{c} < \bar{c}$ such that $\kappa_0(s) \in (\underline{c}, \bar{c})$ for all $s \geq 0$. The result of this section ensures the convergence condition $\lim_{t\to+\infty}(\rho(t), \phi(t)) = (\rho_0, 0)$, even if the curvature is nonconstant, which is a stronger conclusion about (ρ, ϕ) than the ISS condition from Section 2.6.

To prove the result, we define U, $\mathcal{S}$, and $\bar{\Delta}$ as in Theorem 2.5.1, we use the m dynamic extensions

$$\dot{\hat{w}}_i = (\hat{w}_i - \underline{w}_i)(\bar{w}_i - \hat{w}_i)\frac{\cos(\phi)\Phi_i(s)}{(1 + (\rho - \rho_0)\hat{\kappa}(s,t))^2}\frac{\partial U}{\partial \phi}(\rho, \phi) \tag{2.76}$$

having the state space $(\underline{w}_i, \bar{w}_i)$ for $i = 1, \ldots, m$, where

$$\hat{\kappa}_0(s,t) = \sum_{i=1}^{m} \hat{w}_i(t)\Phi_i(s), \tag{2.77}$$

and we define the adaptive controller u_2 from (2.30) except with $\hat{\kappa}_0$ now depending on time t and the arc length s. However, we continue our convention of omitting arguments of functions, when this would not lead to confusion.

Finally, we assume that the known upper and lower bounds $\bar{w}_i$ and $\underline{w}_i$ for the weights w_i in the curvature are such that (2.77) stays in the interval $(\underline{c}, \bar{c})$. Since the unknown parameters are the weights w_i instead of the curvatures $\kappa(s)$ themselves, we use the new augmented errors

$$(\tilde{q}, \tilde{w}) = (\tilde{q}_1, \tilde{q}_2, \tilde{w}) = (\rho - \rho_0, \phi, \hat{w}_1 - w_1, \ldots, \hat{w}_m - w_m), \tag{2.78}$$

which has the same augmented error dynamics we gave in (2.31), except we must now replace the $\tilde{\kappa}_0$ error dynamics by

$$\dot{\tilde{w}}_i = \frac{(w_i + \tilde{w}_i - \underline{w}_i)(\bar{w}_i - w_i - \tilde{w}_i)\Phi_i(s)\cos(\tilde{q}_2)}{(1 + (\rho - \rho_0)\hat{\kappa}_0)^2} \frac{\partial U}{\partial \phi}(\rho, \phi) \tag{2.79}$$

for $i = 1, \ldots, m$, and $\tilde{\kappa}_0 = \hat{\kappa}_0 - \kappa_0$ now takes the form

$$\tilde{\kappa}_0 = \sum_{i=1}^{m} \tilde{w}_i \Phi_i. \tag{2.80}$$

We also use following well known result, called Barbalat's Lemma [17]:

Lemma 2.8.1. *If $\phi : \mathbb{R} \to \mathbb{R}$ is uniformly continuous on $[0, +\infty)$ and*

$$\lim_{t \to +\infty} \int_0^t \phi(m)\, \mathrm{d}m \tag{2.81}$$

exists and is finite, then $\lim_{t \to +\infty} \phi(t) = 0$.

With the preceding changes and $\mathcal{S}^\sharp$ from Theorem 2.5.1 as before, we can then prove the following (but see Remark 2 for cases where we can also identify the curvatures and prove ISS):

Theorem 2.8.1. *Let the assumptions of Theorem 2.5.1 hold with* $\bar{\delta} = 0$. *Then for all solutions* $(\tilde{q}(t), \tilde{w}(t)) = (\rho(t) - \rho_0, \phi(t), \hat{w}_1(t) - w_1, \ldots, \hat{w}_m(t) - w_m)$ *of the augmented error dynamics that start in* $\mathcal{S}_w^\sharp = \{(\tilde{q}, \tilde{w}) : \tilde{q} + (\rho_0, 0) \in \mathcal{S}, \tilde{w}_i \in (\underline{w}_i - w_i, \bar{w}_i - w_i)$ *for all* $i\}$, *the corresponding solutions* $(\tilde{q}(t), \tilde{\kappa}_0(t)) = (\rho(t) - \rho_0, \phi(t), \tilde{\kappa}_0(t))$ *remain in* $\mathcal{S}^\sharp$ *for all* $t \geq 0$ *and are such that* $\lim_{t\to+\infty}(\rho(t), \phi(t)) = (\rho_0, 0)$.

Proof: We indicate the changes needed in the proof of Theorem 2.5.1. Lemma 2.5.1 and its proof remain the same, except with $\tilde{\kappa}$ and $\hat{\kappa}$ also depending on s. Then we change the augmented Lyapunov function to the function

$$U^\sharp : \mathcal{S} \times \prod_{i=1}^{m} (\underline{w}_i - w_i, \bar{w}_i - w_i) \to [0, +\infty) \tag{2.82}$$

that is defined by

$$\begin{aligned} &U^\sharp(\rho, \phi, \tilde{w}) = \\ &U(\rho, \phi) + \sum_{i=1}^{m} \int_0^{\tilde{w}_i} \frac{\ell}{(w_i + \ell - \underline{w}_i)(\bar{w}_i - w_i - \ell)} \mathrm{d}\ell \end{aligned} \tag{2.83}$$

where U is from (2.16). The proof is then the same as the proof of Theorem 2.5.1 (with $\delta = 0$) up through and including (2.44), with the same constant $\beta_0 > 0$. By integrating (2.44) (with the choice $\delta = 0$) on any interval $[0, t]$, this gives

$$\int_0^t \left[(h'(\rho(\ell)) \cos(\phi(\ell)))^2 + \sin^2(\phi(\ell)) \right] \mathrm{d}\ell \;\leq\; \frac{1}{\beta_0} U^\sharp\big(\rho(0), \phi(0), \tilde{w}(0)\big) \tag{2.84}$$

along all trajectories of the closed loop augmented error dynamics contained in $\mathcal{S}^\sharp$. By the forward invariance of $\mathcal{S}^\sharp$ from Lemma 2.5.1, it follows that the function $\mathcal{L}(\ell) = (h'(\rho(\ell)) \cos(\phi(\ell)))^2 + \sin^2(\phi(\ell))$ is uniformly continuous on $\mathcal{S}$. Hence, the result follows from Barbalat's Lemma and our Assumption 1 on h. □

Remark 2. We can use the scaling method from Section 2.7 to enlarge the bounds on the curvatures $\kappa_0(s)$. Also, when the assumptions of Theorem 2.8.1 hold with

$m = 1$, we can use a variant of the last part of the proof of Theorem 2.5.1 to prove that $\lim_{t\to+\infty} \hat{\kappa}_0(s,t) = \kappa_0(s)$ for all s, i.e., we get identification of the nonconstant curvatures. This is done by replacing $V^\sharp$ from (2.45) by

$$V^\sharp(\tilde{q}, \tilde{w}_1) = \bar{\mathcal{M}}_4 U^\sharp(\rho, \phi, \tilde{w}_1) + \tilde{q}_2 \tilde{w}_1 \tag{2.85}$$

for a suitable constant $\bar{\mathcal{M}}_4 > 0$ and assuming that $\Phi_1(s)$ is bounded and admits a uniform positive lower bound $\underline{\Phi} > 0$, i.e., $\Phi_1(s) \geq \underline{\Phi}$ for all $s \geq 0$. Here $U^\sharp$ is the function that we defined in (2.83). To see how this can be done when $\delta = 0$, first notice that Lemma 2.5.1 ensures that we have a constant $\bar{\mathcal{G}}_1^* > 0$ such that

$$\left|\dot{\tilde{w}}_1\right| \leq \bar{\mathcal{G}}_1^* \left|\tilde{q}\right| \quad \text{and} \quad U^\sharp(\rho, \phi, \tilde{w}_1) \geq \frac{|(\tilde{q}, \tilde{w}_1)|^2}{\bar{\mathcal{G}}_1^*} \tag{2.86}$$

on $\mathcal{S}^\sharp$. This gives positive constants $\bar{\mathcal{G}}_2^*$ and $\bar{\mathcal{G}}_3^*$ such that

$$\begin{aligned} \frac{d}{dt}(\tilde{q}_2 \tilde{w}_1) &\leq \Big(h'(\tilde{q}_1 + \rho_0)\cos(\tilde{q}_2) - \mu \sin(\tilde{q}_2) \\ &\quad - \frac{\tilde{w}_1 \cos(\phi)\Phi_1(s)}{(1+\kappa_0(\rho-\rho_0))(1+\hat{\kappa}_0(\rho-\rho_0))}\Big)\tilde{w}_1 + \bar{\mathcal{G}}_1^* |\tilde{q}|^2 \\ &\leq \bar{\mathcal{G}}_2^* (|\tilde{w}_1||\tilde{q}| + |\tilde{q}|^2) - \bar{\mathcal{G}}_3^* \tilde{w}_1^2 \end{aligned}$$

holds on $\mathcal{S}^\sharp$. Then we can argue as in the last part of the proof of Theorem 2.5.1 (with the $\bar{\mathcal{G}}_i$'s replaced by the corresponding $\bar{\mathcal{G}}_i^*$'s, and $\tilde{\kappa}_0$ replaced by $\tilde{w}_1$) to prove that the dynamics for $(\tilde{q}, \tilde{w}_1) = (\rho - \rho_0, \phi, \hat{w}_1 - w_1)$ are GAS with respect to $(0, \mathcal{S}^\sharp)$. Moreover, since the preceding analysis is based on a Lyapunov functional design (instead of the Barbalat's lemma approach from the proof of Theorem 2.8.1), we can extend it to cases with additive uncertainties δ. □

2.9 Examples and Simulations

To illustrate the value of our tracking, parameter identification, and robust forward invariance approach, first consider the special case of Theorem 2.7.1 where $h(\rho) = (\rho - \rho_0)^2$, $\rho_0 = 1$, $\rho_* = 0.25$, $K = 5/4$, $L = 0.4$, and $\mu \in (0, \pi)$ is close enough to

π. Here we use the fact that the right limit requirement $\lim_{\rho\to 0^+} h(\rho) = +\infty$ from Assumption 1 can be omitted; see Section 2.6. Then our condition (2.21) holds, because we have

$$\begin{aligned} &\mu \tan(\mu\rho_*) \geq (0.9\pi)(0.9) > 2.5 > \max\left\{|h'(\rho)| : \rho_* \leq \rho \leq \rho_* + K\rho_0\right\} \\ &= 2\max\{|\rho - 1| : 0.25 \leq \rho \leq 1.5\} = 1.5. \end{aligned} \tag{2.87}$$

Also, the ρ values occurring for points in $\mathcal{S}$ are in $[0.25, 1.5]$, the ϕ values occurring in $\mathcal{S}$ are in $[-\pi/4, \pi/4]$, and we can choose the constant function $\gamma(\ell) = 7.9$, the function $\Gamma(\ell) = 4\ell$, and the constants $\bar{\mathcal{M}}_1 = 5.4$ and $\bar{\mathcal{M}}_2 = 0.5$.

To compute the allowable constants $\bar{\Delta}$ for our perturbation bounds, notice that in terms of our earlier notation, we have $\Delta_* = \min\{|h'(\rho)\cos(\phi)| : (\rho, \phi)^\top \in \text{AB} \cup \text{ED}\} \geq 2\min\{|\rho - 1|/\sqrt{2} : \rho \in [0.25, 0.5] \cup [1.25, 1.5]\} \approx 0.4$ and $\Delta_{**} = \min\{|h'(\rho)\cos(\phi) - \mu\sin(\phi)| : (\rho, \phi)^\top \in \text{BC} \cup \text{EF}\} \approx (1/\sqrt{2})\min\{|2(\rho - 1) - 0.9\pi| : \rho \in [0.25, 1.5]\} \approx \sqrt{2}\min\{|\rho - 2.4| : \rho \in [0.25, 1.5]\} \approx 1.3$. Hence, we choose $\bar{\Delta} = 0.4$. We also choose $\lambda = 1/2$ and the disturbance bound $\bar{\delta} = 2.5$. Since $\underline{c} = 0$, we can omit $1/(\rho_* + (K-1)\rho_0)$ from (2.68)-(2.69); see Remark 1 from Section 2.6.Then our lower bound on $\mathcal{M}_*$ from (2.67) is approximately 13.3.

Hence, since the desired distance to the curve is $\rho_0 = 1$, the upper bound on κ_0 provided by Theorem 2.7.1 is

$$\kappa_0 = \frac{\kappa}{1 + \kappa} < \bar{c} < \frac{2}{3}, \tag{2.88}$$

which corresponds to allowing all constant curvatures $\kappa \in (0, 2)$. If we had instead used Theorem 2.5.1, e.g., with $\lambda = 7/8$, then (2.33)-(2.34) with $\underline{c} = 0$ would have produced the curvature bound $\bar{c} = 0.2$. Therefore, we tripled the bound while also allowing control uncertainties $\delta : [0, +\infty) \to [-2.5, 2.5]$. Also, if we allow nonconstant curvatures, such as curvatures of the form $\kappa^\sharp(s) = \kappa + \eta(s)$ from Section 2.6, then Section 2.6 ensures ISS with respect to the perturbation $\delta(t)$

from (2.56), provided $\kappa \in (0, 2)$ and provided that $|\delta(t)| < \mathcal{M}_* \bar{\Delta} \approx 5.32$, which holds if $\sup_s |\eta(s)| < 5.32$; see (2.56).

We simulated (2.66), using Mathematica and the preceding choices of the parameters and functions, so $\bar{\delta} = 2.5$, the scaling constant is $\mathcal{M}_* = 13.3$, and the curvature bound for $\bar{c}$ is $2/3$. We provide simulations for the cases $\delta(t) = 0$ and then $\delta(t) = 2.5 \sin(t)$ (where δ can represent control uncertainty, or the effects (2.56) of the nonconstant part $\eta(t)$ of the curvature as in the previous paragraph). In our first two simulations, we took $\kappa_0 = 0.5$ (corresponding to the unscaled curvature $\kappa = \kappa_0/(1 - \rho_0 \kappa_0) = 1$, using (2.28)), the scaling constant $\mathcal{M}_* = 13.3$, and the initial value $(\tilde{q}(0), \tilde{\kappa}_0(0)) = (-0.7, \pi/4, 0.15)$ for the augmented error variable, which corresponds to taking the initial value $(\rho(0), \phi(0))$ for the state to be

$$B = \left(\rho_* \left(1 + \frac{1}{\mathcal{M}_*} \right), \mu \rho_* \right) \approx (0.3, 0.8) \tag{2.89}$$

of the corresponding robustly forwardly invariant hexagon and the initial value for the estimated scaled curvature to be $\hat{\kappa}_0(0) = \tilde{\kappa}_0(0) + \kappa_0 = 0.15 + 0.5 = 0.65$, i.e., 30% above the true scaled curvature value $\kappa_0 = 0.5$. Using the relationship (2.28) between κ and κ_0, this corresponds to initializing the estimate $\hat{\kappa}$ of the unscaled curvature at

$$\hat{\kappa}(0) = \frac{\hat{\kappa}_0(0)}{1 - \rho_0 \hat{\kappa}_0(0)} \approx 1.9, \tag{2.90}$$

i.e., approximately twice the actual unscaled curvature value $\kappa = 1$. Figures 2.3 and 2.4 show the corresponding plots for $\tilde{q}_1(t) = \rho(t) - \rho_0$, $\tilde{q}_2(t) = \phi(t)$, and the estimate $\hat{\kappa}(t)$.

In our third simulation, we took the same parameters and disturbance function $\delta(t) = 2.5 \sin(t)$ as in our second simulation, except we changed the initial value $(\rho(0), \phi(0))$ for the state to be the bottom right vertex

$$E = \left(K \rho_0 + \left(1 - \frac{1}{\mathcal{M}_*} \right) \rho_*, -\mu \rho_* \right) \approx (1.5, -0.8) \tag{2.91}$$

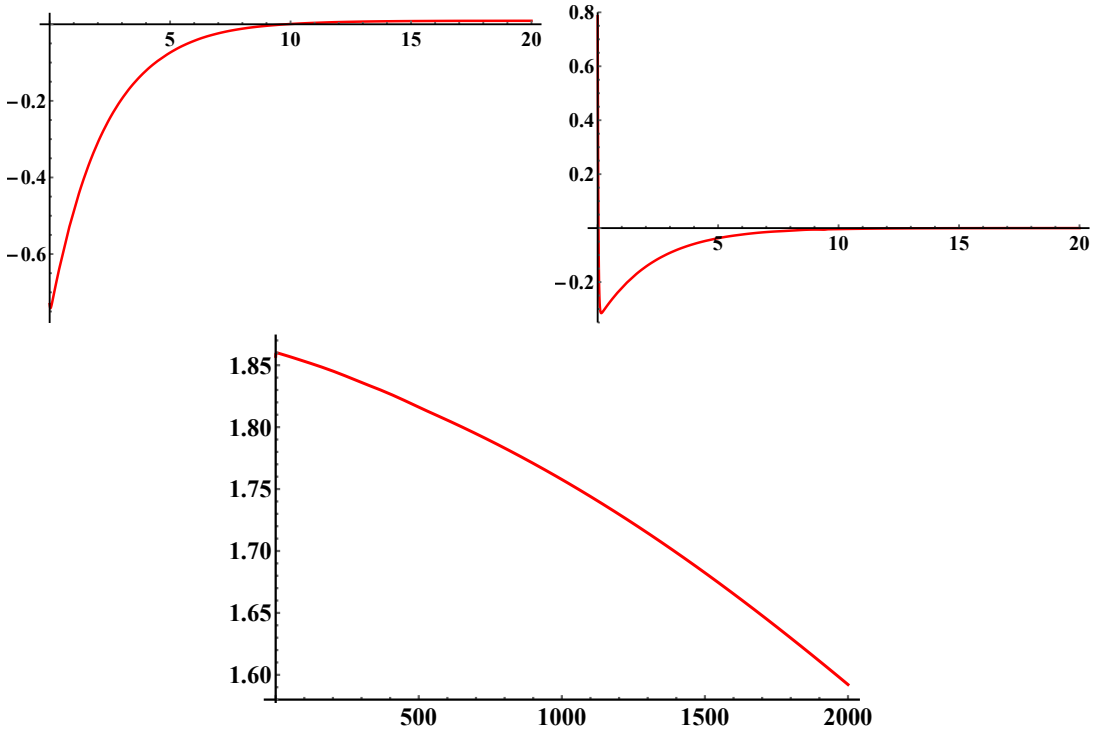

Figure 2.3. Plots from Augmented Error Dynamics (2.66) with Initial Value $(\tilde{q}(0), \tilde{\kappa}_0(0)) = (-0.7, \pi/4, 0.15)$ and $\delta = 0$. (Top Left) $\tilde{q}_1(t) = \rho(t) - \rho_0$, (Top Right) $\tilde{q}_2(t) = \phi(t)$, and (Bottom) $\hat{\kappa}(t)$.

of the corresponding robustly forwardly invariant hexagon. We report results for our third simulation in Figure 2.5, which shows convergence of the state errors towards 0, and the parameter identifiers converging to 1, while staying in the robustly forwardly invariant set $\mathcal{S}^\sharp$, with overshoots from our perturbation in Figures 2.3-2.4. Figure 2.6 shows $(\rho(t), \phi(t)) = (\tilde{q}_1(t) + \rho_0, \tilde{q}_2(t))$ staying in the corresponding set $\mathcal{S}$ for all three simulations. This agrees with our theory.

2.10 Conclusions

Adaptive planar curve tracking under unknown curvatures is important for the control of robots in uncertain environments. While the works [28] and [31] solve adaptive tracking and parameter identification problems under unknown control gains but known curvatures, here we solved a complementary problem, where the control gains are known but where our adaptive controller can cope with unknown curvatures. Our strict Lyapunov function approach allows us to prove input-to-

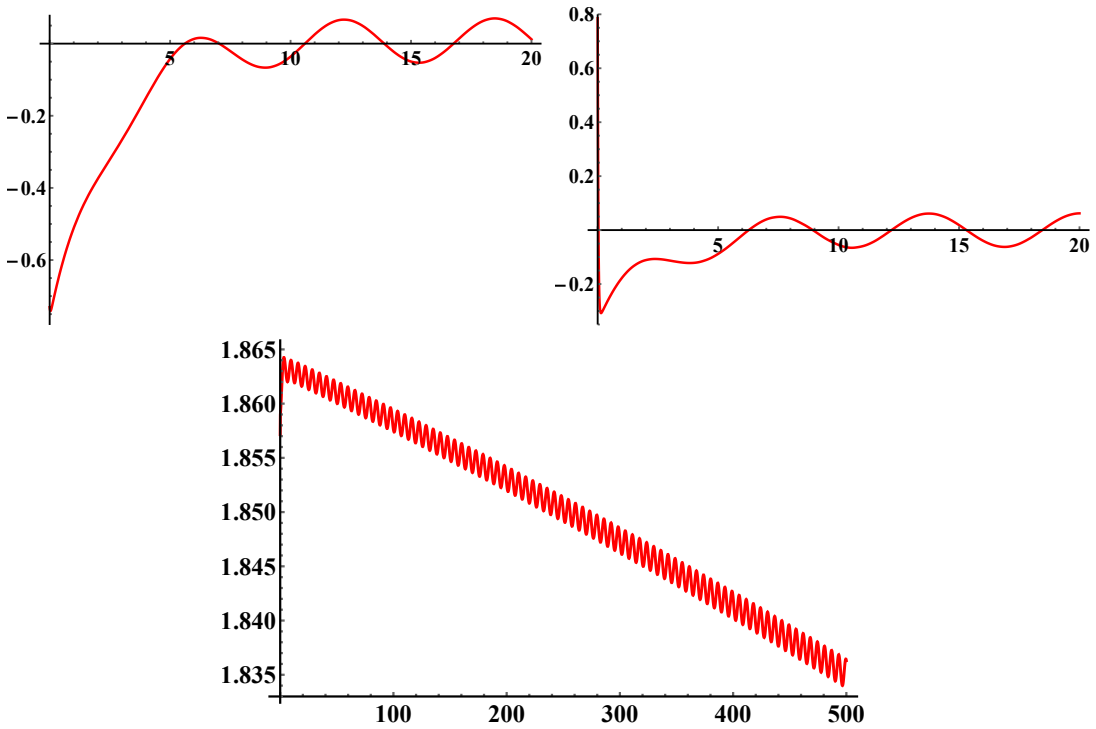

Figure 2.4. Plots from Augmented Error Dynamics (2.66) with Initial Value $(\tilde{q}(0), \tilde{\kappa}_0(0)) = (-0.7, \pi/4, 0.15)$ and $\delta(t) = 2.5\sin(t)$. (Top Left) $\tilde{q}_1(t) = \rho(t) - \rho_0$, (Top Right) $\tilde{q}_2(t) = \phi(t)$, and (Bottom) $\hat{\kappa}(t)$.

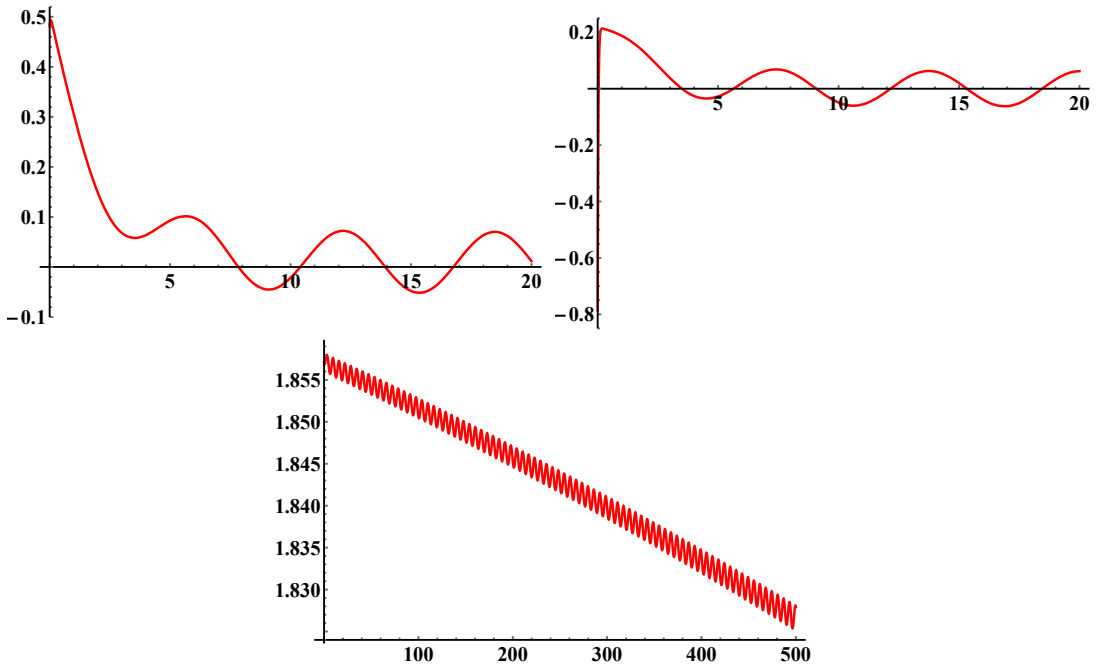

Figure 2.5. Plots from Augmented Error Dynamics (2.66) with Initial Value $(\tilde{q}(0), \tilde{\kappa}_0(0)) = (0.5, -\pi/4, 0.15)$ and $\delta(t) = 2.5\sin(t)$. (Top Left) $\tilde{q}_1(t) = \rho(t) - \rho_0$, (Top Right) $\tilde{q}_2(t) = \phi(t)$, and (Bottom) $\hat{\kappa}(t)$.

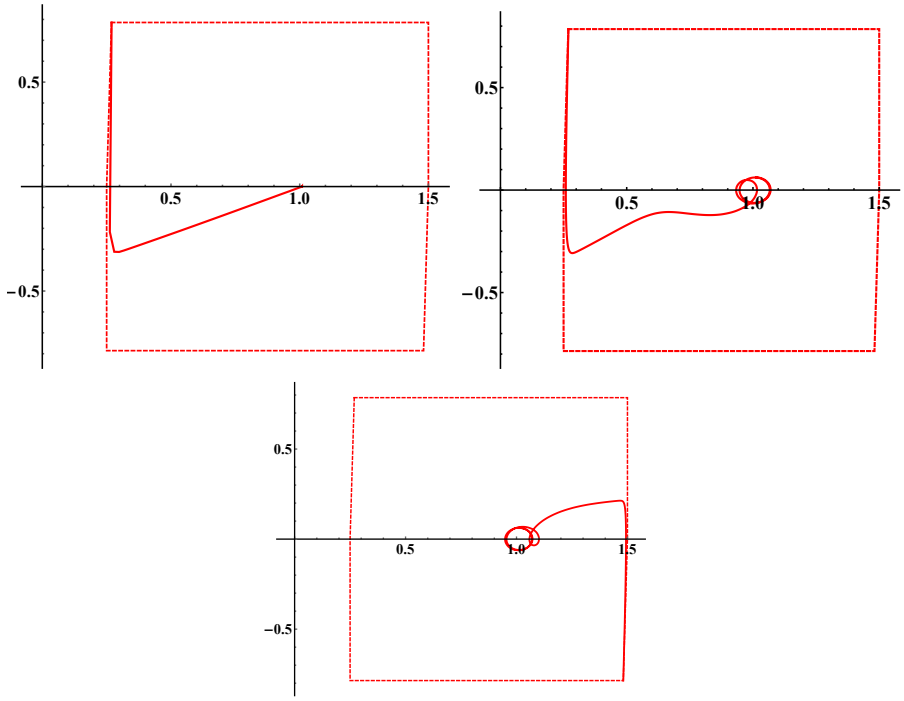

Figure 2.6. States $(\rho(t), \phi(t)) = (\tilde{q}_1(t)+\rho_0, \tilde{q}_2(t))$ Staying in Robustly Forwardly Invariant Set on Time Interval $[0, 20]$ Without Disturbances (Upper Left) and $\delta(t) = 2.5\sin(t)$ (Upper Right and Bottom).

state stability and to cover nonconstant curvatures, and our robust forward invariance approach makes it possible to satisfy a valuable class of polygonal state constraints. One can study even more general three-dimensional cases with input delays, and identify uncertain control gains and uncertain curvatures, using estimators for the unknown curvatures and the unknown control gains. We leave our generalizations for a future work.

Chapter 3
3D Adaptive Curve Tracking

3.1 Background

This chapter provides work from [32] on analogs of the 2D curve tracking results from the previous chapter, except instead of identifying unknown curvatures, here we use our adaptive tracking and parameter identification approach to identify unknown control gains. It is important to identify unknown control gains, because the gains provide a useful measure of the control effectiveness. The 3D case was explored in the work [31], where instead of having hexagons in the plane, the tracking, input-to-state stability with respect to additive uncertainties on the control, and the robust forward invariance was achieved using paired hexagons.

A key observation from [31, Remark 2] is that for fixed penalty functions in the control and a fixed desired bounding set $\mathcal{D}$ for the allowable values of the perturbations, one can build the hexagon pairs (depending on $\mathcal{D}$ and the control) to ensure robust forward invariance of the hexagon pairs under all $\mathcal{D}$ valued perturbations. However, a potential drawback was that larger $\mathcal{D}$'s led to robustly forwardly invariant hexagon pairs that include points that are very close to the boundary of the workspace, as well as points that correspond to the robot being very far from the curve being tracked, and an analogous statement holds for 2D curve tracking. Since this can allow robots to move close to undesirable regions, it can be a disadvantage.

To help overcome the preceding challenge in the 2D case, the previous chapter and [33] used a scaling algorithm that can be summarized as follows. The scaling made it possible to compensate for the effects of arbitrarily large perturbation bounds. First, we fixed any suitable 2D hexagon shaped compact region $\mathcal{H}$ in the workspace and a value $\bar{\delta} > 0$ for the perturbation bound. Then, we scaled the steering constant and the penalty functions in the control by a constant $\mathcal{M}_* \geq 1$

(depending on $\mathcal{H}$ and $\bar{\delta}$) and proved robust forward invariance of $\mathcal{H}$ for the closed loop system under all scalar perturbations that are bounded by $\bar{\delta}$. This eliminated the need to move the hexagon legs too close or far from the boundary of the workspace, and can help ensure robust, safe operation under perturbations.

In this chapter, we extend the 2D scaling approach from our work [33] to the 3D curve tracking dynamics from [31], to ensure tracking under control uncertainty and state constraints and identification of unknown control gains under arbitrarily large perturbation bounds using adaptive control. As in [33], a benefit of the new method in this chapter is that it eliminates the need to include points in the hexagons that may be too close to the boundary of the state space. However, while [33] used only one scaling constant, our 3D dynamics will lead us to use three different scaling constants. We can extend this approach to cover input delays, by converting our strict Lyapunov functions into Lyapunov-Krasovskii functionals, using ideas from [31, Section 7.4]. The effects of input delays can be captured by the perturbation terms using a variant of [31, Section 6.3] that we leave to the reader.

3.1.1 Model and Controls

To make our work more self contained, we review the 3D curve tracking model and robust forward invariant sets from [31]. Then we present our new work, starting in Section 3.2. The model describes the motion of a free particle, and a second particle (called the closest or projection point) that is confined to a specified 3D curve and that locally has the shortest distance to the free particle. Let $\mathbf{r_1}$ be the position of the second particle, $\mathbf{x_1}$ be the unit tangent vector to the curve at $\mathbf{r_1}$, $\mathbf{y_1}$ be a unit normal vector, and $\mathbf{z_1}$ be a binormal. The velocity of the point is in the direction of $\mathbf{x_1}$.

Let $\mathbf{r_2}$ be the position of the free particle moving at unit speed, $\mathbf{x_2}$ be the unit tangent vector to the trajectory of its moving center, $\mathbf{y_2}$ be a corresponding unit normal vector, and $\mathbf{z_2} = \mathbf{x_2} \times \mathbf{y_2}$. With the speed $\frac{ds}{dt} = \alpha$, the dynamics of the free point and the closest point on the curve from [31] and [52] are

$$\begin{aligned} \dot{\mathbf{r}}_1 &= \alpha \mathbf{x_1} & \dot{\mathbf{r}}_2 &= \mathbf{x_2} \\ \dot{\mathbf{x}}_1 &= \alpha\kappa_n \mathbf{y_1} + \alpha\kappa_g \mathbf{z_1} & \dot{\mathbf{x}}_2 &= u\mathbf{y_2} + v\mathbf{z_2} \\ \dot{\mathbf{y}}_1 &= -\alpha\kappa_n \mathbf{x_1} & \dot{\mathbf{y}}_2 &= -u\mathbf{x_2} \\ \dot{\mathbf{z}}_1 &= -\alpha\kappa_g \mathbf{x_1}, & \dot{\mathbf{z}}_2 &= -v\mathbf{x_2}, \end{aligned} \tag{3.1}$$

where the normal curvature κ_n and the geodesic curvature κ_g are associated with the curve at the closest point, and the steering controls u and v we will chosen later. See Figure 3.1 below.

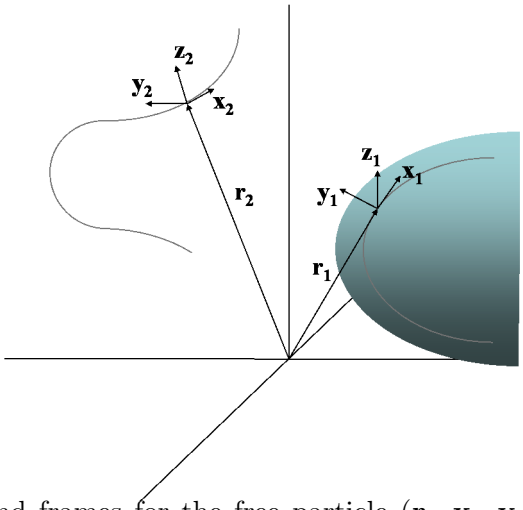

Figure 3.1. Position and frames for the free particle $(\mathbf{r_2}, \mathbf{x_2}, \mathbf{y_2}, \mathbf{z_2})$ and shadow point $(\mathbf{r_1}, \mathbf{x_1}, \mathbf{y_1}, \mathbf{z_1})$ [52].

Following [31], we write the controls as

$$\begin{aligned} u &= a_1(\mathbf{x_1} \cdot \mathbf{y_2}) + a_2(\mathbf{y_1} \cdot \mathbf{y_2}) + a_3(\mathbf{z_1} \cdot \mathbf{y_2}) \quad \text{and} \\ v &= a_1(\mathbf{x_1} \cdot \mathbf{z_2}) + a_2(\mathbf{y_1} \cdot \mathbf{z_2}) + a_3(\mathbf{z_1} \cdot \mathbf{z_2}), \end{aligned} \tag{3.2}$$

where the coefficients a_i will be specified. We also set $\rho_1 = (\mathbf{r_2} - \mathbf{r_1}) \cdot \mathbf{y_1}$ and $\rho_2 = (\mathbf{r_2} - \mathbf{r_1}) \cdot \mathbf{z_1}$, and we use the shape variables $\varphi = \mathbf{x_1} \cdot \mathbf{x_2}$, $\beta = \mathbf{y_1} \cdot \mathbf{x_2}$, and

$\gamma = \mathbf{z_1} \cdot \mathbf{x_2}$, and the spherical coordinate transformation

$$(\varphi, \beta, \gamma) = \big(\cos(\zeta)\cos(\theta), -\sin(\zeta)\cos(\theta), \sin(\theta)\big). \tag{3.3}$$

Finally, we choose

$$a_1 = \mu, \;\; a_2 = -h_1'(\rho_1) + \frac{\alpha\kappa_n}{\varphi} \text{ and } a_3 = -h_2'(\rho_2) + \frac{\alpha\kappa_g}{\varphi}, \tag{3.4}$$

where $\mu > 0$ is any fixed constant (and called the steering constant) and the C^1 penalty functions $h_i : (0, +\infty) \to [0, +\infty)$ are

$$h_i(\rho_i) = \begin{cases} \bar{h}_i \left(\rho_i + \dfrac{\rho_{ci}^2}{\rho_i} - 2\rho_{ci} \right), & \rho_i \in (0, \rho_{ci}) \\ \dfrac{\bar{h}_i}{\rho_{ci}} (\rho_i - \rho_{ci})^2, & \rho_i \geq \rho_{ci} \end{cases} \tag{3.5}$$

for $i = 1, 2$ for fixed constants $\bar{h}_i > 0$ and $(\rho_{c1}, \rho_{c2}) \in (0, +\infty)^2$, and we assume that κ_n and κ_g are C^1, bounded, and nonpositive valued. Then

$$\alpha = \frac{\varphi}{1 - \kappa_n \rho_1 - \kappa_g \rho_2}, \tag{3.6}$$

as noted in [31]. This is a slight generalization of the controls from [31], which required that $\bar{h}_1 = \bar{h}_2$. Our basic tracking goal is to ensure that

$$\lim_{t \to +\infty} (\rho_1, \zeta, \rho_2, \theta)(t) = (\rho_{c1}, 0, \rho_{c2}, 0) \tag{3.7}$$

for all initial conditions, to ensure parallel motion relative to the curve that is being tracked while maintaining sufficient separation between the robot and the curve [31]. Our state constraints will ensure that the ρ_i's and φ stays positive.

Using [31, Section 5.2] (except with different $\bar{h}_i$ used in the penalty functions h_i) with the control components (3.4) scaled by $G/\hat{G}$, we obtain the augmented

adaptive 3D curve tracking dynamics with parameter estimate $\hat{G}$ given by

$$\begin{aligned}
\dot{\rho}_1 &= -\sin(\zeta)\cos(\theta) \\
\dot{\zeta} &= -\frac{\cos(\zeta)\kappa_n}{1-\kappa_n\rho_1-\kappa_g\rho_2}\frac{1}{\cos(\theta)}\left(\frac{G}{\hat{G}}-\cos^2(\theta)\right)-\frac{\alpha\kappa_g\sin(\theta)\sin(\zeta)}{\cos(\theta)} \\
&\quad +\frac{G}{\hat{G}}\frac{h_1'(\rho_1)\cos(\zeta)}{\cos(\theta)}-\frac{G}{\hat{G}}\frac{\mu\sin(\zeta)}{\cos(\theta)}+\delta_1 \\
\dot{\rho}_2 &= \sin(\theta) \\
\dot{\theta} &= -\frac{\kappa_g\cos^2(\zeta)\cos(\theta)}{1-\kappa_n\rho_1-\kappa_g\rho_2}+\frac{G}{\hat{G}}\left(-h_1'(\rho_1)\right. \\
&\quad \left.+\frac{\kappa_n}{1-\kappa_n\rho_1-\kappa_g\rho_2}\right)\sin(\zeta)\sin(\theta) \\
&\quad +\left[\frac{G}{\hat{G}}\left(-h_2'(\rho_2)+\frac{\kappa_g}{1-\kappa_n\rho_1-\kappa_g\rho_2}\right)\cos(\theta)\right] \\
&\quad -\frac{G}{\hat{G}}\mu\cos(\zeta)\sin(\theta)+\delta_2 \\
\dot{\hat{G}} &= \frac{(g_{\max}-\hat{G})(\hat{G}-g_{\min})}{\hat{G}}\left(\frac{\partial U}{\partial\zeta}\mathcal{A}_1(Y)+\frac{\partial U}{\partial\theta}\mathcal{A}_2(Y)\right)
\end{aligned} \tag{3.8}$$

on the augmented state space

$$\mathcal{X}_a = (0,+\infty)\times(-\pi/2,\pi/2)\times(0,+\infty)\times(-\pi/2,\pi/2)\times(g_{\min},g_{\max}), \tag{3.9}$$

where the unknown measurable essentially bounded functions δ_i represent uncertainty, G is an unknown control gain (i.e., an unknown positive constant that multiplies the control components in the system) that is known to lie on some interval $(g_{\min}, g_{\max})$ with known positive endpoints $g_{\min}$ and $g_{\max}$, the functions $\mathcal{A}_i(Y)$ of the state $Y=(\rho_1,\zeta,\rho_2,\theta)$ are

$$\begin{aligned}
\mathcal{A}_1(Y) &= -\frac{1}{\cos(\theta)}\left[\left(\frac{\kappa_n}{1-\kappa_n\rho_1-\kappa_g\rho_2}-h_1'(\rho_1)\right)\cos(\zeta)\right. \\
&\quad \left.+\mu\sin(\zeta)\right], \quad \text{and} \\
\mathcal{A}_2(Y) &= -\mu\cos(\zeta)\sin(\theta) \\
&\quad +\left(\frac{\kappa_n}{1-\kappa_n\rho_1-\kappa_g\rho_2}-h_1'(\rho_1)\right)\sin(\zeta)\sin(\theta) \\
&\quad +\left(\frac{\kappa_g}{1-\kappa_n\rho_1-\kappa_g\rho_2}-h_2'(\rho_2)\right)\cos(\theta),
\end{aligned} \tag{3.10}$$

where Y is valued in $\mathcal{X} = (0, +\infty) \times (-\pi/2, \pi/2) \times (0, +\infty) \times (-\pi/2, \pi/2)$, and

$$\begin{aligned} &U(\rho_1, \zeta, \rho_2, \theta) = \\ &-h_1'(\rho_1)\sin(\zeta)\cos(\theta) + h_2'(\rho_2)\sin(\theta) + \textstyle\int_0^{V(\rho_1,\zeta,\rho_2,\theta)} \mathcal{L}_0(q)\mathrm{d}q, \end{aligned} \tag{3.11}$$

where

$$V(\rho_1, \zeta, \rho_2, \theta) \;=\; -\ln(\cos(\theta)) - \ln(\cos(\zeta)) + h_1(\rho_1) + h_2(\rho_2) \tag{3.12}$$

and

$$\mathcal{L}_0(q) \;=\; \frac{3}{\mu}\big[\Gamma(q) + 1\big]\big(1 + |\kappa_n|_\infty + |\kappa_g|_\infty\big) + 2\left[\frac{1}{\mu}\lambda(q) + \Gamma'(q) + 1\right], \tag{3.13}$$

and $\lambda(q) = \lambda_0(q, \rho_{c1}) + \lambda_0(q, \rho_{c2}) + 2\bar{c}/\min\{\rho_{c1}, \rho_{c2}\}$ and $\Gamma(q) = \Gamma_0(q, \rho_{c1}) + \Gamma_0(q, \rho_{c2}) + 4\bar{c}q/\min\{\rho_{c1}, \rho_{c2}\}$, with the choices $\bar{c} = \max\{\bar{h}_1, \bar{h}_2\}$ and

$$\begin{aligned} &\lambda_0(q, \rho_{ci}) = \frac{2}{\bar{c}^2\rho_{ci}^4}(q + 2\bar{c}\rho_{ci})^3 + 1 + 0.5(\mu)^2 + \mu \\ &\text{and } \Gamma_0(q, \rho_{ci}) = \frac{18\bar{c}}{\rho_{ci}}q + \left(\frac{2}{\rho_{ci}}\right)^4 \frac{9q^4}{\bar{c}^2}\,. \end{aligned} \tag{3.14}$$

When the parameter estimate $\hat{G}$ for the unknown parameter G is equal to G, our system (3.8) can be written as [31]

$$\begin{aligned} \dot{\rho}_1 &= -\sin(\zeta)\cos(\theta) \\ \dot{\zeta} &= \delta_1 - \frac{1}{\cos^2(\theta)}\big[\alpha\kappa_n\sin^2(\theta) + \alpha\kappa_g\sin(\theta)\sin(\zeta)\cos(\theta) \\ &\quad -h_1'(\rho_1)\cos(\zeta)\cos(\theta) + \mu\sin(\zeta)\cos(\theta)\big] \\ \dot{\rho}_2 &= \sin(\theta) \\ \dot{\theta} &= \alpha\kappa_g\frac{\sin^2(\zeta)}{\cos(\zeta)} - h_2'(\rho_2)\cos(\theta) - \mu\cos(\zeta)\sin(\theta) + \delta_2 \\ &\quad + \left(-h_1'(\rho_1) + \frac{\alpha\kappa_n}{\cos(\theta)\cos(\zeta)}\right)\sin(\zeta)\sin(\theta) \end{aligned} \tag{3.15}$$

on the state space $\mathcal{X} = (0, +\infty) \times (-\pi/2, \pi/2) \times (0, +\infty) \times (-\pi/2, \pi/2)$, which we call the nonadaptive dynamics, and in the special case where the perturbations δ_i are identically zero in (3.15), we call (3.15) the unperturbed nonadaptive dynamics. The motivation for (3.11) is that U is a strict Lyapunov function

for the unperturbed nonadaptive dynamics on $\mathcal{X}$ with respect to its equilibrium $\mathcal{E} = (\rho_{c1}, 0, \rho_{c2}, 0)$; see [31, Theorem 2]. The barrier term $(g_{\max} - \hat{G})(\hat{G} - g_{\min})$ in (3.8) ensures that the parameter estimate $\hat{G}$ stays in the interval $(g_{\min}, g_{\max})$ that contains G. We can use a variant of the proof of [31, Theorem 5] (with a scaling of the h_i's by different constants $\bar{h}_i$, and with the δ_i's set equal to 0) to show this curve tracking and parameter identification result:

Theorem 3.1.1. *When the δ_i's are zero, the dynamics (3.8) are uniformly globally asymptotically stable to the equilibrium $(\rho_{c1}, 0, \rho_{c2}, 0, G)$ on its state space $\mathcal{X}_a = (0, +\infty) \times (-\pi/2, \pi/2) \times (0, +\infty) \times (-\pi/2, \pi/2) \times (g_{\min}, g_{\max})$.* □

3.1.2 Robust Forward Invariance

The preceding subsection leaves open the problem of finding largest possible perturbation sets $\mathcal{D} \subseteq \mathbb{R}^2$ such that all solutions of the Y subsystem in (3.8), for all measurable essentially bounded choices of $\delta = (\delta_1, \delta_2) : [0, +\infty) \to \mathcal{D}$, that start in suitable subsets $\mathcal{H}$ of $\mathcal{X}$ remain in $\mathcal{H}$ at all future times. In [31], we solved the preceding robust forward invariant problem by choosing the sets $\mathcal{H} \subseteq \mathcal{X}$ to be paired hexagons and the allowable perturbation sets to be compact subsets of maximal boxes $\mathcal{D}$. The $\mathcal{D}$'s were maximal in the sense that for each constant perturbation $\bar{d}$ that takes a value outside $\mathcal{D}$, there existed a point p_* on the boundary of $\mathcal{H}$ such that the corresponding solution of the nonadaptive dynamics (3.15) starting at p_* for the perturbation $\bar{d}$ exits $\mathcal{H}$ in finite time. The analysis in [31] assumes that $\bar{h}_1 = \bar{h}_2$, but it carries over to the case where these constants can differ.

Given any quadruple $(\rho_{*1}, \rho_{*2}, K_1, K_2) \in (0, \rho_{c1}) \times (0, \rho_{c2}) \times [\rho_{c1}, +\infty) \times [\rho_{c2}, +\infty)$ and any constants $\bar{\zeta} \in (0, \pi/2)$ and $\bar{\theta} \in (0, \pi/2)$, the robustly forwardly invariant sets in [31] took the form$\mathcal{H} = H_1(\rho_{*1}, \bar{\zeta}, K_1) \times H_2(\rho_{*2}, \bar{\theta}, K_2)$, where $H_1(\rho_{*1}, \bar{\zeta}, K_1)$ is the closed set in the (ρ_1, ζ) plane whose boundary is the hexagon that has the

vertices $A = (\rho_{*1}, 0)$, $B = (\rho_{*1} + \bar{\zeta}/\mu^\sharp, \bar{\zeta})$, $C = (\rho_{*1} + 2\bar{\zeta}/\mu^\sharp + K_1, \bar{\zeta})$, $D = (\rho_{*1} + 2\bar{\zeta}/\mu^\sharp + K_1, 0)$, $E = (\rho_{*1} + \bar{\zeta}/\mu^\sharp + K_1, -\bar{\zeta})$, and $F = (\rho_{*1}, -\bar{\zeta})$, and $H_2(\rho_{*2}, \bar{\theta}, K_2)$ is the closed set in the (ρ_2, θ) plane whose boundary is the hexagon with the vertices $A' = (\rho_{*2}, 0)$, $B' = (\rho_{*2}, \bar{\theta})$, $C' = (\rho_{*2} + \bar{\theta}/(\mu^\sharp \cos(\bar{\zeta})) + K_2, \bar{\theta})$,$D' = (\rho_{*2} + 2\bar{\theta}/(\mu^\sharp \cos(\bar{\zeta})) + K_2, 0)$, $E' = (\rho_{*2} + 2\bar{\theta}/(\mu^\sharp \cos(\bar{\zeta})) + K_2, -\bar{\theta})$, and $F' = (\rho_{*2} + \bar{\theta}/(\mu^\sharp \cos(\bar{\zeta})), -\bar{\theta})$, where $\mu^\sharp = \mu g_{\min}/g_{\max}$, and the corresponding perturbation sets had the form $\mathcal{D} = [-\delta_{*1}, \delta_{*1}] \times [-\delta_{*2}, \delta_{*2}]$ for suitable maximum constant bounds δ_{*i} for $i = 1$ and 2. See Figure 3.2.

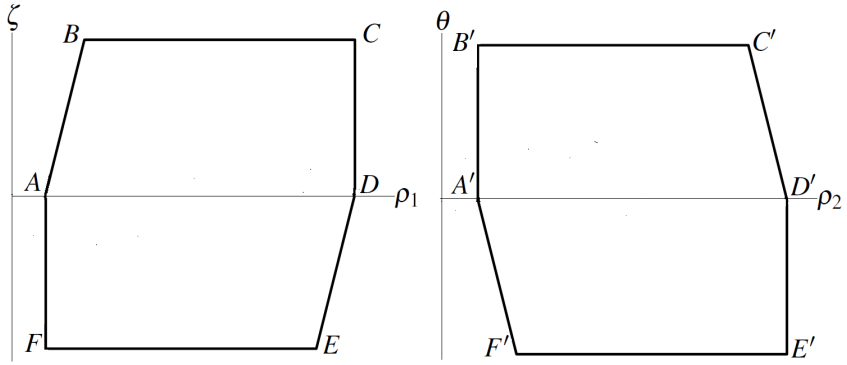

Figure 3.2. Hexagon Shaped Boundaries of Two-Dimensional Sets $H_1(\rho_{*1}, \bar{\zeta}, K_1)$ (Left) and $H_2(\rho_{*2}, \bar{\theta}, K_2)$ (Right) for Robustly Forwardly Invariant Set $H_1(\rho_{*1}, \bar{\zeta}, K_1) \times H_2(\rho_{*2}, \bar{\theta}, K_2)$

Also, [31, Remark 2] showed that for each pair $(\delta_{*1}, \delta_{*2}) \in (0, +\infty)$, we can chose the K_i's and ρ_{*i}'s and μ such that $\mathcal{H}$ is robustly forwardly invariant for the dynamics (3.15) with the perturbation set $\mathcal{D}$. However, as the δ_{*i}'s become large, the required ρ_{*i}'s converge to 0, and the required K_i's converge to $+\infty$, which may be a disadvantage, since small ρ_{*i}'s correspond to allowing the robot to get very close to the curve, and large K_i's allow the robot to get very far from the curve. Our new results that we present next help overcome this disadvantage.

3.2 Robust Forward Invariance under Scaling

The remainder of this work is new theory that has not appeared previously and substantially differs from [31]. Since the barrier term $(g_{\max} - \hat{G})(\hat{G} - g_{\min})$ in (3.8)

keeps the parameter estimate $\hat{G}$ in the interval $(g_{\min}, g_{\max})$ [31], and since there are no perturbations in the parameter update law

$$\dot{\hat{G}} = (g_{\max} - \hat{G})(\hat{G} - g_{\min})\frac{1}{\hat{G}}\left(\frac{\partial U}{\partial \zeta}\mathcal{A}_1(Y) + \frac{\partial U}{\partial \theta}\mathcal{A}_2(Y)\right) \tag{3.16}$$

from (3.8), it suffices to prove robust forward invariance for the $Y = (\rho_1, \zeta, \rho_2, \theta)$ subsystem of (3.8) on subsets of

$$\mathcal{X} = (0, +\infty) \times (-\pi/2, \pi/2) \times (0, +\infty) \times (-\pi/2, \pi/2) \tag{3.17}$$

for each choice of $\hat{G}(t)$. To this end, we first rewrite this Y subsystem as

$$\begin{cases} \dot{\rho}_1 &= -\sin(\zeta)\cos(\theta) \\ \dot{\zeta} &= \mathcal{Q}_1(Y, \hat{G}, \mu, \bar{h}) + \delta_1 \\ \dot{\rho}_2 &= \sin(\theta) \\ \dot{\theta} &= \mathcal{Q}_2(Y, \hat{G}, \mu, \bar{h}) + \delta_2, \end{cases} \tag{3.18}$$

where

$$\begin{aligned} \mathcal{Q}_1(Y, \hat{G}, \mu, \bar{h}) = &-\frac{\cos(\zeta)\kappa_n}{1 - \kappa_n\rho_1 - \kappa_g\rho_2}\frac{1}{\cos(\theta)}\left(\frac{G}{\hat{G}} - \cos^2(\theta)\right) \\ &-\frac{\alpha\kappa_g \sin(\theta)\sin(\zeta)}{\cos(\theta)} + \frac{G}{\hat{G}}\frac{h_1'(\rho_1)\cos(\zeta)}{\cos(\theta)} - \frac{G}{\hat{G}}\frac{\mu\sin(\zeta)}{\cos(\theta)} \end{aligned} \tag{3.19}$$

and

$$\begin{aligned} \mathcal{Q}_2(Y, \hat{G}, \mu, \bar{h}) = &-\frac{\kappa_g\cos^2(\zeta)\cos(\theta)}{1 - \kappa_n\rho_1 - \kappa_g\rho_2} \\ &+\frac{G}{\hat{G}}\left(-h_1'(\rho_1) + \frac{\kappa_n}{1 - \kappa_n\rho_1 - \kappa_g\rho_2}\right)\sin(\zeta)\sin(\theta) \\ &+\frac{G}{\hat{G}}\left(-h_2'(\rho_2) + \frac{\kappa_g}{1 - \kappa_n\rho_1 - \kappa_g\rho_2}\right)\cos(\theta) - \frac{G\mu\cos(\zeta)\sin(\theta)}{\hat{G}}, \end{aligned} \tag{3.20}$$

where we leave out the dependencies of the $\mathcal{Q}_i$'s on t (through the time-varying curvatures κ_n and κ_g) to simplify the notation. The preceding functions agree with the $\mathcal{Q}_i^{\mathcal{A}}$'s in [31], but we write them as $\mathcal{Q}_i(Y, \hat{G}, \mu, \bar{h})$'s to emphasize their dependence on the constant choices of μ and $\bar{h} = (\bar{h}_1, \bar{h}_2)$.

However, unlike in [31] where we computed the maximum allowable bounds for the perturbations to maintain forward invariance of

$$\mathcal{H} = H_1(\rho_{*1}, \bar{\zeta}, K_1) \times H_2(\rho_{*2}, \bar{\theta}, K_2), \tag{3.21}$$

here we do the following. First, we fix a disturbance set

$$\bar{\mathcal{D}} = [-\bar{\Delta}_1, \bar{\Delta}_1] \times [-\bar{\Delta}_2, \bar{\Delta}_2] \tag{3.22}$$

that is known to contain all $\delta(t)$ values, where the $\bar{\Delta}_i$'s are any known nonnegative constants. Then, we choose μ and the $\bar{h}_i$'s to ensure that (3.21) is robustly forwardly invariant for (3.18) with perturbations $\delta : [0, +\infty) \to \bar{\mathcal{D}}$, where the constants $\rho_{*i} \in (0, \rho_{ci})$ and $K_i \in [\rho_{ci}, +\infty)$ for $i = 1, 2$, $\bar{\zeta} \in (0, \pi/2)$, and $\bar{\theta} \in (0, \pi/2)$ are fixed; see Section 3.3 below for a detailed comparison between the method in [31] and the one we provide here, including algorithms for applying both methods.

Enlarging μ increases the slopes of the tilted legs AB and DE in Figure 3.2 and decreases the slopes of the legs A′F′ and C′D′, so our new hexagons have the same general shape as in Figure 3.2 but become more like boxes. Also, for each constant $\bar{\mu} \geq 1$, we have

$$\begin{aligned}
(\rho_{c1}, 0) &\in H_1(\rho_{*1}, \bar{\zeta}, K_1) \\
&\subseteq \left[\rho_{*1}, \rho_{*1} + \frac{2\bar{\zeta}}{\bar{\mu}} + K_1\right] \times [-\bar{\zeta}, \bar{\zeta}] \text{ and} \\
(\rho_{c2}, 0) &\in H_2(\rho_{*2}, \bar{\theta}, K_2) \\
&\subseteq \left[\rho_{*2}, \rho_{*2} + \frac{2\bar{\theta}}{\bar{\mu}\cos(\bar{\zeta})} + K_2\right] \times [-\bar{\theta}, \bar{\theta}]
\end{aligned} \tag{3.23}$$

for all choices of

$$\mu^\sharp = \mu \frac{g_{\min}}{g_{\max}} \geq \bar{\mu}, \tag{3.24}$$

so the hexagons maintain a positive distance of $\min\{\rho_{*1}, \rho_{*2}, \pi/2 - \bar{\zeta}, \pi/2 - \bar{\theta}\}$ from the boundary of $\mathcal{X}$ for all choices of $\mu^\sharp \geq \bar{\mu}$. On the other hand, it is impossible to prove robust forward invariance of boxes instead of hexagons; see [31, Remark 4].

Our new robust forward invariance result will follow from this analogue of [31, Lemma 4], which will lead to our new robust forward invariance algorithm in Section 3.3:

Theorem 3.2.1. *Let* $(\rho_{*1}, \rho_{*2}, K_1, K_2, \bar{\zeta}, \bar{\theta}, \bar{\Delta}_1, \bar{\Delta}_2) \in (0, \rho_{c1}) \times (0, \rho_{c2}) \times [\rho_{c1}, +\infty) \times [\rho_{c2}, +\infty) \times (0, \pi/2)^2 \times [0, +\infty)^2$ *be any constant vector. Then we can choose the constants* $\bar{h}_i > 0$ *in the penalty functions* h_i *in (3.5), and the constant* $\mu \geq 1$ *in (3.4), such that the following four conditions E1-E4 are satisfied:*

E1 $\mathcal{Q}_1(Y, \hat{G}, \mu, \bar{h}) + \mu^\sharp \sin(\zeta)\cos(\theta) > \bar{\Delta}_1$ *for all* $(\rho_1, \zeta) \in ED$ *and all* $(\rho_2, \theta) \in H_2(\rho_{*2}, \bar{\theta}, K_2)$. *Also,* $\mathcal{Q}_1(Y, \hat{G}, \mu, \bar{h}) + \mu^\sharp \sin(\zeta)\cos(\theta) < -\bar{\Delta}_1$ *for all* $(\rho_1, \zeta) \in AB$ *and all* $(\rho_2, \theta) \in H_2(\rho_{*2}, \bar{\theta}, K_2)$.

E2 $\mathcal{Q}_1(Y, \hat{G}, \mu, \bar{h}) > \bar{\Delta}_1$ *for all* $(\rho_1, \zeta) \in FE$ *and all* $(\rho_2, \theta) \in H_2(\rho_{*2}, \bar{\theta}, K_2)$. *Also,* $\mathcal{Q}_1(Y, \hat{G}, \mu, \bar{h}) < -\bar{\Delta}_1$ *for all* $(\rho_1, \zeta) \in BC$ *and all* $(\rho_2, \theta) \in H_2(\rho_{*2}, \bar{\theta}, K_2)$.

E3 $\mathcal{Q}_2(Y, \hat{G}, \mu, \bar{h}) + \mu^\sharp \cos(\bar{\zeta})\sin(\theta) > \bar{\Delta}_2$ *for all* $(\rho_2, \theta) \in A'F'$ *and all* $(\rho_1, \zeta) \in H_1(\rho_{*1}, \bar{\zeta}, K_1)$. *Also,* $\mathcal{Q}_2(Y, \hat{G}, \mu, \bar{h}) + \mu^\sharp \cos(\bar{\zeta})\sin(\theta) < -\bar{\Delta}_2$ *for all* $(\rho_2, \theta) \in C'D'$ *and all* $(\rho_1, \zeta) \in H_1(\rho_{*1}, \bar{\zeta}, K_1)$.

E4 $\mathcal{Q}_2(Y, \hat{G}, \mu, \bar{h}) > \bar{\Delta}_2$ *for all* $(\rho_2, \theta) \in F'E'$ *and all* $(\rho_1, \zeta) \in H_1(\rho_{*1}, \bar{\zeta}, K_1)$. *Also,* $\mathcal{Q}_2(Y, \hat{G}, \mu, \bar{h}) < -\bar{\Delta}_2$ *for all* $(\rho_2, \theta) \in B'C'$ *and all* $(\rho_1, \zeta) \in H_1(\rho_{*1}, \bar{\zeta}, K_1)$.

hold for all values $\hat{G} \in (g_{\min}, g_{\max})$ *of the parameter estimate for the unknown control gain* G. □

Proof. The proof has the same structure as the proof of [31, Lemma 4], except instead of reducing the ρ_{*i}'s and increasing the K_i's to make E1-E4 hold as was done in [31], we choose μ and the $\bar{h}_i$'s big enough. However, the changes needed in the proofs from [31] are significant, so we provide a complete proof here. We

assume that

$$\mu > \frac{g_{\max}}{g_{\min}} \max\left\{ \frac{\bar{\zeta}}{\rho_{c1}-\rho_{*1}}, \bar{\zeta}, \frac{\bar{\theta}}{\cos(\bar{\zeta})}, \frac{\bar{\theta}}{\cos(\bar{\zeta})(\rho_{c2}-\rho_{*2})} \right\} . \tag{3.25}$$

Later we put more restrictions on μ.We first place conditions on $\bar{h}_1 \geq 1$ such that E1 holds for all μ's that satisfy (3.25).

Since (3.25) gives $\mu^\sharp = \mu g_{\min}/g_{\max} > \bar{\zeta}/(\rho_{c1}-\rho_{*1})$, we have $\rho_1 \leq \rho_{*1}+\bar{\zeta}/\mu^\sharp < \rho_{c1}$ on the leg AB. Also, $\zeta \geq 0$ on AB, the h_i''s are nondecreasing, and $h_1''(\rho_{c1}) > 0$. Therefore, at all points $Y = (\rho_1, \zeta, \rho_2, \theta) \in H_1(\rho_{*1}, \bar{\zeta}, K_1) \times H_2(\rho_{*2}, \bar{\theta}, K_2)$ such that $(\rho_1, \zeta) \in AB$ and for all values $\hat{G} \in [g_{\min}, g_{\max}]$, we have $h_1'(\rho_1) \leq h_1'(\rho_{*1}+\bar{\zeta}/\mu^\sharp) < 0$, and so

$$\begin{aligned}
&\mathcal{Q}_1(Y, \hat{G}, \mu, \bar{h}) + \mu^\sharp \sin(\zeta)\cos(\theta) \\
&= -\frac{\cos(\zeta)\kappa_n}{1-\kappa_n\rho_1-\kappa_g\rho_2}\frac{1}{\cos(\theta)}\left(\frac{G}{\hat{G}} - \cos^2(\theta)\right) - \frac{\alpha\kappa_g \sin(\theta)\sin(\zeta)}{\cos(\theta)} \\
&+ \frac{G h_1'(\rho_1)\cos(\zeta)}{\hat{G}\cos(\theta)} - \left\{ \frac{\sin(\zeta)\mu}{\cos(\theta)}\left(\frac{G}{\hat{G}} - \cos^2(\theta)\frac{g_{\min}}{g_{\max}}\right)\right\} \\
&\leq \frac{1}{\cos(\theta)}\left[|\kappa_n|_\infty \left(\frac{g_{\max}}{g_{\min}} + 1\right) + |\kappa_g|_\infty \right. \\
&\left. + \frac{g_{\min}\cos(\bar{\zeta}) h_1'(\rho_{*1}+\bar{\zeta}/\mu^\sharp)}{g_{\max}}\right] \;<\; -\bar{\Delta}_1 \,,
\end{aligned} \tag{3.26}$$

when $\bar{h}_1 \geq 1$ is large enough, using the nonnegativity of the term in curly braces in (3.26) along AB, the nonpositivity of the curvatures which implies that

$$|\alpha| = \frac{|\varphi|}{1-\kappa_n\rho_1-\kappa_g\rho_2} \leq 1 \tag{3.27}$$

and the fact that $0 < \cos(\bar{\zeta}) \leq \cos(\zeta) \leq 1$ on $H_1(\rho_{*1}, \bar{\zeta}, K_1) \times H_2(\rho_{*2}, \bar{\theta}, K_2)$, to use $h_1'(\rho_{*1}+\bar{\zeta}/\mu^\sharp) < 0$ to cancel the effects of the other terms in (3.26). The proof that

$$\mathcal{Q}_1(Y, \hat{G}, \mu, \bar{h}) + \mu^\sharp \sin(\zeta)\cos(\theta) > \bar{\Delta}_1 \tag{3.28}$$

at all points $(\rho_1, \zeta) \in DE$ for large enough $\bar{h}_1 \geq 1$ is analogous, because for all such points, we can use our assumption that $K_1 \geq \rho_{c1}$ to get $h_1'(\rho_1) \geq h_1'(\rho_{*1} +$

$\bar{\zeta}/\mu^\sharp + K_1) > 0$, and the fact that $\zeta \leq 0$ on the leg DE and nonpositivity of the term in curly braces in (3.26). This provides our conditions on $\bar{h}_1$ to satisfy E1, which hold for all μ's that satisfy (3.25).

Next, we specify $\bar{h}_2$'s such that E3 holds for all $\mu \geq 1$ that satisfy (3.25). Along $A'F'$, condition (3.25) and our choice of the vertex F$'$ give

$$\rho_2 \leq \rho_{*2} + \frac{\bar{\theta}}{\mu^\sharp \cos(\bar{\zeta})} < \rho_{c2}, \tag{3.29}$$

so

$$h_2'(\rho_2) \leq h_2'(\rho_{*2} + \bar{\theta}/[\mu^\sharp \cos(\bar{\zeta})]) < 0 \tag{3.30}$$

(because our formulas (3.5) for the h_i's imply that h_2' is nondecreasing, $h_2'(\rho_{c2}) = 0$, and $h_2''(\rho_{c2}) > 0$). Also, $-\pi/2 < \theta \leq 0$ and so $\sin(\theta) \leq 0$ for all pairs (ρ_2, θ) on $A'F'$. Hence,

$$\begin{aligned}
&\mathcal{Q}_2(Y, \hat{G}, \mu, \bar{h}) + \mu^\sharp \cos(\bar{\zeta}) \sin(\theta) \\
&= -\frac{\kappa_g \cos^2(\zeta)\cos(\theta)}{1 - \kappa_n\rho_1 - \kappa_g\rho_2} + \frac{G}{\hat{G}}\left(-h_1'(\rho_1) + \frac{\kappa_n}{1 - \kappa_n\rho_1 - \kappa_g\rho_2}\right)\sin(\zeta)\sin(\theta) \\
&+ \frac{G}{\hat{G}}\left(-h_2'(\rho_2) + \frac{\kappa_g}{1 - \kappa_n\rho_1 - \kappa_g\rho_2}\right)\cos(\theta) \\
&+ \left\{\mu \sin(\theta)\left(-\frac{G}{\hat{G}}\cos(\zeta) + \frac{g_{\min}}{g_{\max}}\cos(\bar{\zeta})\right)\right\} \\
&\geq -|\kappa_g|_\infty + \frac{g_{\min}}{g_{\max}}\left|h_2'\left(\rho_{*2} + \frac{\bar{\theta}}{\mu^\sharp \cos(\bar{\zeta})}\right)\right|\cos(\bar{\theta}) \\
&- \frac{g_{\max}}{g_{\min}}\left(\sin(\bar{\theta})|h_1'|_{[\rho_{*1}, \rho_{*1}+K_1+2]} + \sin(\bar{\theta})|\kappa_n|_\infty + |\kappa_g|_\infty\right) \;>\; \bar{\Delta}_2
\end{aligned} \tag{3.31}$$

at all points $Y \in H_1(\rho_{*1}, \bar{\zeta}, K_1) \times H_2(\rho_{*2}, \bar{\theta}, K_2)$ such that (ρ_2, θ) is on the leg $A'F'$, when $\bar{h}_2 \geq 1$ is large enough (where the lower bound on allowable $\bar{h}_2$'s depends on the choice of $\bar{h}_1$, but not on the choice of μ that satisfies (3.25)), since the term in curly braces in (3.31) is nonnegative at such points. To get the inequality in (3.31),

we also used the fact that $\mu^\sharp > \bar{\zeta}$, which follows from (3.25) and implies that

$$\rho_{*1} \leq \rho_1 \leq \rho_{*1} + K_1 + 2 \tag{3.32}$$

for all $(\rho_1, \zeta) \in H_1(\rho_{*1}, \bar{\zeta}, K_1)$. Analogous reasoning gives the other assertion in E3, because the term in curly braces in (3.31) is nonpositive on $C'D'$. Finally, enlarging $\mu \geq 1$ gives conditions E2 and E4. □

The proof that Theorem 3.2.1 leads to our desired robust forward invariance result for the paired hexagons can now be done using the following analog of the proof of [31, Theorem 3] that we gave in [31]. We introduce the constants

$$\begin{aligned}
&\Delta_a^* = \min_{\hat{G}}\{|\mathcal{Q}_1(Y, \hat{G}, \mu, \bar{h}) + \mu^\sharp \sin(\zeta)\cos(\theta)| : \\
&(\rho_1, \zeta) \in AB \cup ED, (\rho_2, \theta) \in H_2(\rho_{*2}, \bar{\theta}, K_2)\}, \\
&\Delta_b^* = \min_{\hat{G}}\{|\mathcal{Q}_1(Y, \hat{G}, \mu, \bar{h})| : (\rho_1, \zeta) \in FE \cup BC, (\rho_2, \theta) \in H_2(\rho_{*2}, \bar{\theta}, K_2)\}, \\
&\Delta_c^* = \min_{\hat{G}}\{|\mathcal{Q}_2(Y, \hat{G}, \mu, \bar{h}) + \mu^\sharp \cos(\bar{\zeta})\sin(\theta)| : \\
&(\rho_2, \theta) \in C'D' \cup A'F', (\rho_1, \zeta) \in H_1(\rho_{*1}, \bar{\zeta}, K_1)\}, \text{ and} \\
&\Delta_d^* = \min_{\hat{G}}\{|\mathcal{Q}_2(Y, \hat{G}, \mu, \bar{h})| : (\rho_2, \theta) \in B'C' \cup F'E', (\rho_1, \zeta) \in H_1(\rho_{*1}, \bar{\zeta}, K_1)\},
\end{aligned}$$

where the subscript $\hat{G}$ means that the minimization is also over all constants $\hat{G} \in [g_{\min}, g_{\max}]$.Then

$$\min\{\Delta_a^*, \Delta_b^*\} \geq \bar{\Delta}_1 \text{ and } \min\{\Delta_c^*, \Delta_d^*\} \geq \bar{\Delta}_2, \tag{3.33}$$

where $\bar{\Delta}_i$ is the known bound on $|\delta_i(t)|$ for $i = 1, 2$ as before, and our results apply for any choices $\bar{\Delta}_i \geq 0$. Set

$$\bar{\Delta}_\zeta = \min\{\Delta_a^*, \Delta_b^*\} \text{ and } \bar{\Delta}_\theta = \min\{\Delta_c^*, \Delta_d^*\}. \tag{3.34}$$

The following implies that our adaptive tracking and parameter identification dynamics (3.8) has the robustly forwardly invariant set $H_1(\rho_{*1}, \bar{\zeta}, K_1) \times H_2(\rho_{*2}, \bar{\theta}, K_2) \times (g_{\min}, g_{\max})$ for suitable perturbation sets $\mathcal{D}$:

Corollary 3.2.1. *Let* $(\bar{\zeta}, \bar{\theta}) \in (0, \pi/2)^2$, $(\bar{\Delta}_1, \bar{\Delta}_2) \in [0, +\infty)^2$, *and* $(\rho_{*1}, \rho_{*2}, K_1, K_2) \in (0, \rho_{c1}) \times (0, \rho_{c2}) \times [\rho_{c1}, +\infty) \times [\rho_{c2}, +\infty)$ *be given constants, and choose any constant vector* $(\mu, \bar{h}_1, \bar{h}_2)$ *such that conditions E1-E4 from Lemma 3.2.1 hold. Then: (a) For each* C^1 *solution* $\hat{G} : [0, +\infty) \to (g_{\min}, g_{\max})$ *of the update law (3.16) and all constants* $\delta_{*1} \in (0, \bar{\Delta}_\zeta)$ *and* $\delta_{*2} \in (0, \bar{\Delta}_\theta)$, *the set*

$$\mathcal{H} = H_1(\rho_{*1}, \bar{\zeta}, K_1) \times H_2(\rho_{*2}, \bar{\theta}, K_2) \tag{3.35}$$

is robustly forwardly invariant for (3.18) with the disturbance set $\mathcal{D} = [-\delta_{*1}, \delta_{*1}] \times [-\delta_{*2}, \delta_{*2}]$. *(b) For each constant* $\delta_+ > \bar{\Delta}_\zeta$ *(resp.,* $> \bar{\Delta}_\theta$*), there exist a boundary point* $Y \in \partial(H_1(\rho_{*1}, \bar{\zeta}, K_1) \times H_2(\rho_{*2}, \bar{\theta}, K_2))$ *and a solution of (3.16) such that the trajectory for (3.18) starting at* Y *for one of the constant perturbations* $\pm(\delta_+, 0)$ *(resp.,* $\pm(0, \delta_+)$*) exits* $H_1(\rho_{*1}, \bar{\zeta}, K_1) \times H_2(\rho_{*2}, \bar{\theta}, K_2)$ *in finite time.* □

Proof. The proof of Corollary 3.2.1 has the same structure as the proof of [31, Theorem 3], with the important difference that instead of using conditions (C1)-(C4) from [31, Lemma 4], we use the corresponding conditions E1 and E3 (resp., E2 and E4) to prevent trajectories from exiting through the tilted (resp., top and bottom) legs of the paired hexagons. □

By combining Theorem 3.1.1 and Corollary 3.2.1, we can prove that for all constants $\bar{\Delta}_i \geq 0$ for $i = 1, 2$ and each choice of $\mathcal{D}$ that satisfies the requirements from Corollary 3.2.1, the system (3.8) is input-to-state stable with respect to its equilibrium $(\rho_{c1}, 0, \rho_{c2}, 0, G)$ on each set

$$H_1(\rho_{*1}, \bar{\zeta}, K_1) \times H_2(\rho_{*2}, \bar{\theta}, K_2) \times (g_{\min}, g_{\max}) \tag{3.36}$$

with perturbations $\delta = (\delta_1, \delta_2)$ that are valued in $\mathcal{D}$. This follows from the boundedness of the gradient of U on any of the compact paired hexagons, and [31, Lemma 2]. This implies curve tracking and identification of the control gain G, in

the special case where the perturbations δ_i are 0. We next compare the preceding algorithm with the algorithm from [31] in detail.

3.3 Comparing Algorithms

Section 3.2 provides a very different way to find tolerance and safety bounds from the method in [31, Remark 2]. To see why, we first express the method from [31, Remark 2] as follows, where the legs refer to those of $H_1(\rho_{*1}, \bar{\zeta}, K_1) \times H_2(\rho_{*2}, \bar{\theta}, K_2)$ from Figure 3.2 above, as before:

Algorithm 1. Given any positive constants $\bar{\Delta}_i$ such that the unknown perturbation δ_i in (3.8) is known to take all of its values in $[-\bar{\Delta}_i, \bar{\Delta}_i]$ for $i = 1$ and 2, any pairs $(\rho_{c1}, \rho_{c2}) \in (0, +\infty)^2$ and $(\bar{\zeta}, \bar{\theta}) \in (0, \pi/2)^2$, and any common value

$$c = \bar{h}_1 = \bar{h}_2 > 0 \tag{3.37}$$

for the constants in the formula (3.5) for the penalty functions h_i, choose the constants $\mu > 0$ and $\rho_{*i} \in (0, \rho_{ci})$ and $K_i > 0$ for $i = 1$ and 2 using these steps:

S1 Choose $\mu > 0$ and constants $\bar{\rho}_{*i} \in (0, \rho_{ci})$ for $i = 1, 2$ such that (3.25) holds for all $\rho_{*i} \in (0, \bar{\rho}_{*i})$ for $i = 1, 2$.

S2 Choose $\rho_{*1} \in (0, \bar{\rho}_{*1})$ small enough and $K_1 \geq \rho_{c1}$ large enough such that for all μ satisfying S1, we have:

G1 $\mathcal{Q}_1(Y, \hat{G}, \mu, \bar{h}) + \mu^\sharp \sin(\zeta) \cos(\theta) < -\bar{\Delta}_1$ (resp., $> \bar{\Delta}_1$) at all points on the leg AB (resp., DE).

S3 Choose $\rho_{*2} \in (0, \bar{\rho}_{*2})$ small enough and $K_2 \geq \rho_{c2}$ large enough such that for all μ satisfying S1, we have:

G2 $\mathcal{Q}_2(Y, \hat{G}, \mu, \bar{h}) + \mu^\sharp \cos(\bar{\zeta}) \sin(\theta) > \bar{\Delta}_2$ (resp., $< -\bar{\Delta}_2$) at all points on the leg A′F′ (resp., C′D′).

S4 Enlarge $\mu > 0$ as needed to satisfy E2 and E4.

Then $H_1(\rho_{*1}, \bar{\zeta}, K_1) \times H_2(\rho_{*2}, \bar{\theta}, K_2) \times (g_{\min}, g_{\max})$ is robustly forwardly invariant for the augmented system (3.8) for all disturbances δ valued in $\mathcal{D} = [-\bar{\Delta}_1, \bar{\Delta}_1] \times [-\bar{\Delta}_2, \bar{\Delta}_2]$. □

While not explicitly stated in [31], Algorithm 1 follows from the proof of [31, Lemma 4] and uses the properties

$$\lim_{\rho_i \to 0^+} h_i(\rho_i) = \lim_{\rho_i \to +\infty} h_i(\rho_i) = +\infty \tag{3.38}$$

for $i = 1, 2$ to pick the ρ_{*i}'s small enough and the K_i's big enough. The choices of ρ_{*2} and K_2 in Step S3 depend on the choices of ρ_{*1} and K_1 from Step S2. If we use Algorithm 1, then larger perturbation bounds $\bar{\Delta}_i$ require choosing smaller positive constants ρ_{*i} and larger K_i's, so the hexagons get close to the vertical axes in Figure 3.2, and also become wider (which corresponds to allowing the robot to move far from the curve being tracked).

By contrast, our new algorithm from Section 3.2 is as follows, where conditions G1-G2 are from Algorithm 1:

Algorithm 2. Given any positive constants $\bar{\Delta}_i$ such that the unknown perturbation δ_i in (3.8) is known to take all of its values in $[-\bar{\Delta}_i, \bar{\Delta}_i]$ for $i = 1$ and 2, any pairs $(\rho_{c1}, \rho_{c2}) \in (0, +\infty)^2$ and $(\bar{\zeta}, \bar{\theta}) \in (0, \pi/2)^2$, and any constants $\rho_{*i} \in (0, \rho_{ci})$ and $K_i \geq \rho_{ci}$ for $i = 1$ and 2, choose the constant $\mu > 0$ and the scaling constants $\bar{h}_i$'s in (3.5) as follows:

M1 Choose any constant $\mu > 0$ such that (3.25) holds.

M2 Choose $\bar{h}_1$ such that G1 holds for all μ satisfying (3.25).

M3 Choose $\bar{h}_2$ such that G2 holds for all μ satisfying (3.25).

M4 Enlarge $\mu > 0$ as needed to satisfy E2 and E4.

Then $H_1(\rho_{*1}, \bar{\zeta}, K_1) \times H_2(\rho_{*2}, \bar{\theta}, K_2) \times (g_{\min}, g_{\max})$ is robustly forwardly invariant for the augmented system (3.8) for all disturbances δ valued in $\mathcal{D} = [-\bar{\Delta}_1, \bar{\Delta}_1] \times [-\bar{\Delta}_2, \bar{\Delta}_2]$. □

Since $\mathcal{Q}_2(Y, \hat{G}, \mu, \bar{h}) + \mu^\sharp \cos(\bar{\zeta}) \sin(\theta)$ depends on h_1, the $\bar{h}_2$ in Step M3 will depend on $\bar{h}_1$. Algorithm 2 scales the h_i's by increasing the $\bar{h}_i$'s, instead of using the approach from Algorithm 1 of manipulating the arguments of the h_i's. Algorithm 2 eliminates the need to allow the paired hexagons to get too wide or close to the vertical axes in Figure 3.2, which is helpful in applications that require separation between the robot and the curve being tracked; see (3.23). By proving ISS under arbitrarily large $\bar{\Delta}_i$'s, under scalings of μ and of the $\bar{h}_i$'s, while maintaining positive distances between the paired hexagons and the edges of the state space, our work also improves on the ISS results from [31], which did not use our scaling approach and did not compensate for arbitrarily large disturbances unless the distances from the paired hexagons to the edges of the state space decreased towards zero.

3.4 Conclusions

We advanced the theory of state constrained 3D curve tracking by exploiting connections between tuning constants and allowable perturbation bounds that ensure robust forward invariance. Our new results include perturbations, polygonal state constraints, and identification of unknown control gains using adaptive control. Our scaling approach tunes scaling constants in the controls to compensate for arbitrarily large disturbance bounds while maintaining desirable separation between the polygons and the edges of the state space, and so builds on [31, Remark 2] from the recent *SIAM Journal on Control and Optimization* paper by Malisoff and Zhang.

Chapter 4
Summary of Results and Future Work

This dissertation advanced the theory of 2D and 3D curve tracking, using novel synergies of Lyapunov functions, robust forward invariance, and adaptive tracking and parameter identification, including cases where the unknown parameters to be identified enter the dynamics in a nonlinear way. While robustness properties had been previously observed in field work involving the types of gyroscopic controls that we used in this work, our robust forward invariance method provided a new way to quantify the effects of uncertainties in terms of input-to-state stability and to compute nonconservative bounds on the allowable additive uncertainties on the controls that ensure robust forward invariance of the corresponding hexagons in the robust forward decomposition of the state spaces. This is valuable because collision avoidance problems in robotics call for computing tolerance and safety bounds to ensure safe operation of robots when obstacles are present.

In our future work, we hope to find analogs of our 2D curve tracking results for other engineering models in which the unknown parameters enter in a nonlinear way, and to allow 2D curve tracking cases where there are both unknown curvatures and unknown control gains. We are not aware of any general method to achieve adaptive tracking and parameter identification for systems where the parameters to be identified enter the system in a nonlinear way. See [26] for model reference adaptive control systems where the unknown parameters are products of unknown weight and control effectiveness matrices which enter in a quadratic way and where the estimators converge to the true parameter values.Our Mathematica simulations in the 2D case exhibited convergence of the parameter estimates to the unknown parameter that was much slower than the convergence of the tracking error to zero. Therefore, we are also motivated to search for ways to accelerate the rate of the

parameter identification, without sacrificing the fast convergence of the tracking error to zero.

The 3D curve tracking case leads to paired hexagons and two curvatures, namely, the geodesic curvature and the normal curvature. It would be of interest to develop analogs of our 2D curve tracking curvature identification results that make it possible to identify both of the curvatures in the 3D case. Our research group's original results [31] on the 3D curve case also covered input delays, i.e., cases where the current state of the system is not available for measurement, which would necessitate using time lagged values of the states instead of current values in the feedback controls. It is valuable to include the effects of input delays, because in field work with marine robots, it may be the case that the control is being computed remotely (e.g., using an on-shore computer, instead of on the marine robot itself) which produces communication delays between the sensors on the robot and the device being used to compute the control values; see, e.g., our research group's marine robotic field work as described in [40]. The strategy in [31] for compensating for the delays was to incorporate the effects of the delays into the additive uncertainties on the control. However, there is a large literature on delay compensation that is based on other techniques, such as the reduction model method, and sequential predictors; see [3, 8, 35] and the survey article [16]. In future work, we hope to compare the performance of different possible delay compensation methods in our curve tracking controls, by comparing rates of convergence of the tracking and parameter identification errors that are obtained using different delay compensation methods.

References

[1] A. Aguiar and J. Hespanha. Trajectory tracking and path-following of underactuated autonomous vehicles with parametric modeling uncertainty. *IEEE Transactions on Automatic Control*, 52(8):1362-1379, 2007. doi: 10.1109/TAC.2007.902731.

[2] P. Albertos and I. Mareels. *Feedback and Control for Everyone*. Springer, New York, 2010.

[3] Z. Artstein. Linear systems with delayed controls: a reduction. *IEEE Transactions on Automatic Control*, 27(4):869-879, 1982. 10.1109/TAC.1982.1103023.

[4] K. Astrom and B. Witternmark. *Adaptive Control, Second Edition*. Prentice Hall, Upper Saddle River, NJ, 1994.

[5] J-P. Aubin and H. Frankowska. *Set-Valued Analysis*. Birkhauser, Boston, 2009.

[6] A. Bacciotti and L. Rosier. *Liapunov Functions and Stability in Control Theory, Second Edition*. Springer-Verlag, Berlin, 2005.

[7] M. Bardi and I. Capuzzo-Dolcetta. *Optimal Control and Viscosity Solutions of Hamilton-Jacobi-Bellman Equations*. Birkhauser, Boston, MA, 1997.

[8] G. Besancon, D. Georges, and Z. Benayache. Asymptotic state prediction for continuous-time systems with delayed input and application to control. In *Proceedings of the European Control Conference (Kos, Greece, 2-5 July 2007)*, pp. 1786-1791.

[9] E. Borhaug and K. Pettersen. Adaptive way-point tracking control for underactuated autonomous vehicles. In *Proceedings of the 44th IEEE Conference on Decision and Control (Seville, Spain, 12-15 December 2005)*, pp. 4028–4034. doi: 10.1109/CDC.2005.1582792.

[10] D. Bresch-Pietri and M. Krstic. Delay-adaptive predictor feedback for systems with unknown long actuator delay. *IEEE Transactions on Automatic Control*, 55(9):2106–2112, 2010. doi: 10.1109/TAC.2010.2050352.

[11] D. Bresch-Pietri and M. Krstic. Delay-adaptive control for nonlinear systems. *IEEE Transactions on Automatic Control*, 59(5):1203–1218, 2014. doi: 10.1109/TAC.2014.2298711.

[12] K. Do, Z-P. Jiang, and J. Pan. Robust adaptive path following of underactuated ships. *Automatica* 40(6):929-944, 2004. doi: 10.1016/j.automatica.2004.01.021.

[13] K. Do and J. Pan. Robust path-following of underactuated ships: Theory and experiments on a model ship. *Ocean Engineering*, 33(10):1354–1372. doi: 10.1016/j.oceaneng.2005.07.011.

[14] M. Hirsch, S. Smale, and R. Devaney. *Differential Equations, Dynamical Systems, and an Introduction to Chaos, Third Edition*. Academic Press, New York, 2013.

[15] E. Justh and P. Krishnaprasad. Natural frames and interacting particles in three dimensions. In *Proceedings of the 44th IEEE Conference on Decision and Control and European Control Conference (Seville, Spain, 12-15 December 2005)*, pp. 2841-2846. doi: 10.1109/CDC.2005.1582594.

[16] I. Karafyllis, M. Malisoff, F. Mazenc, and P. Pepe. Stabilization of nonlinear delay systems: A tutorial on recent results. In *Recent Results on Nonlinear Delay Control Systems*, I. Karafyllis, M. Malisoff, F. Mazenc, and P. Pepe, Eds., Advances in Delays and Dynamics Series Vol. 4, Springer, New York, 2016, pp. 1-41. doi: 10.1007/978-3-319-18072-4_1.

[17] H. Khalil. *Nonlinear Systems, Third Edition*. Prentice Hall, Upper Saddle River, NJ, 2002.

[18] M. Krstic. *Delay Compensation for Nonlinear, Adaptive, and PDE Systems*. Birkhauser, Boston, MA, 2009.

[19] M. Krstic, I. Kanellakopoulos, and P. Kokotovic. *Nonlinear and Adaptive Control Design*. John Wiley and Sons, New York, 1995.

[20] M. Krstic and A. Smyshlyaev. Adaptive control of PDEs. *Annual Reviews in Control*, 32:149-160, 2008. doi: 10.1016/j.arcontrol.2008.05.001.

[21] E. Lefeber, K. Pettersen, and H. Nijmeijer. Tracking control of an underactuated ship. *IEEE Transactions on Control Systems Technology*, 11(1):52-61, 2003. doi: 10.1109/TCST.2002.806465.

[22] R. Lenain, B. Thuilot, C. Cariou, and P. Martinet. High accuracy path tracking for vehicles in presence of sliding: Application to farm vehicle automatic guidance for agricultural tasks. *Autonomous Robots*, 21(1):79-97, 2006. doi: 10.1007/s10514-006-7806-4.

[23] V. Lumelsky and A. Stepanov. Path planning strategies for a point mobile automaton moving amidst unknown obstacles of arbitrary shape. *Algorithmica*, 2(1-4):403–430, 1987. doi: 10.1007/BF01840369.

[24] M. Malisoff and F. Mazenc. Constructions of Strict Lyapunov Functions. Springer, London, UK, 2009.

[25] M. Malisoff, F. Mazenc, and F. Zhang. Stability and robustness analysis for curve tracking control using input-to-state stability. *IEEE Transactions on Automatic Control*, 57:1320-1326, 2012. doi: 10.1109/TAC.2011.2174664.

[26] M. Malisoff, S. Sarsilmaz, T. Yucelen, and J. Muse. Tracking, parameter identification, and convergence rates for model reference adaptive control. In *Proceedings of the American Control Conference (Milwaukee, WI, 27-29 June 2018)*, to appear. https://www.math.lsu.edu/∼malisoff/.

[27] M. Malisoff and E. Sontag. Asymptotic controllability and input-to-state stabilization: The effect of actuator errors. In *Optimal Control, Stabilization, and Nonsmooth Analysis*, M. de Queiroz, M. Malisoff, and P. Wolenski, Eds., Lecture Notes in Control and Information Sciences Vol. 301, Springer-Verlag, New York, 2004, pp. 155-171.

[28] M. Malisoff and F. Zhang. Adaptive control for planar curve tracking under controller uncertainty. *Automatica*, 49(5):1411-1418, 2013. doi: 10.1016/j.automatica.2013.01.056.

[29] M. Malisoff and F. Zhang. Robustness of a class of three-dimensional curve tracking control laws under time delays and polygonal state constraints. In *Proceedings of the American Control Conference (Washington, DC, 17-19 June 2013)*, pp. 5710-5715. doi: 10.1109/ACC.2013.6580729.

[30] M. Malisoff and F. Zhang. An adaptive control design for 3D curve tracking based on robust forward invariance. In *Proceedings of the 52nd IEEE Conference on Decision and Control (Florence, Italy, 10-13 December 2013)*, pp. 4473-4478. doi: 10.1109/CDC.2013.6760578.

[31] M. Malisoff and F. Zhang. Robustness of adaptive control under time delays for three-dimensional curve tracking. *SIAM Journal on Control and Optimization*, 53(4):2203-2236, 2015. doi: 10.1137/120904354.

[32] M. Malisoff, R. Sizemore, and F. Zhang. Robustness of adaptive control for three-dimensional curve tracking under state constraints: effects of scaling control terms. In *Proceedings of the 55th IEEE Conference on Decision and Control (Las Vegas, NV, 12-14 December 2016)*, pp. 3825-3830. doi: 10.1109/CDC.2016.7798846.

[33] M. Malisoff, R. Sizemore, and F. Zhang. Adaptive planar curve tracking control and robustness analysis under state constraints and unknown curvature. *Automatica*, 75:133-143, 2017. doi: 10.1016/j.automatica.2016.09.017.

[34] F. Mazenc and M. Malisoff. Strict Lyapunov function constructions under LaSalle conditions with an application to Lotka-Volterra systems. *IEEE Transactions on Automatic Control*, 55(4):841-854, 2010. doi: 10.1109/TAC.2010.2041995.

[35] F. Mazenc and M. Malisoff. Stabilization and robustness analysis for time-varying systems with time-varying delays using a sequential subpredictors approach. *Automatica*, 82:118-127, 2016. doi: 10.1016/j.automatica.2017.04.020.

[36] F. Mazenc, G. Robledo, and M. Malisoff. Stability and robustness analysis for a multispecies chemostat model with delays in the growth rates and uncertainties. *Discrete and Continuous Dynamical Systems Series B*, 23(4):1851-1872, 2018. doi: 10.3934/dcdsb.2018098.

[37] A. Micaelli and C. Samson. Trajectory tracking for unicycle-type and two-steering-wheels mobile robots. *INRIA Report 2097*, 1993. https://hal.inria.fr/inria-00074575/PDF/RR-2097.pdf.

[38] P. Morin and C. Samson. Motion control of wheeled mobile robots. In *Springer Handbook of Robotics*. Springer, Berlin, Germany. pp. 799–826, 2008. doi: 10.1007/978-3-540-30301-5_35.

[39] S. Mukhopadhyay, C. Wang, S. Bradshaw, V. Bazie, S. Maxon, L. Hicks, M. Patterson, and F. Zhang. Controller performance of marine robots in reminiscent oil surveys. In *Proceedings of the 2012 IEEE/RSJ International Conference on Intelligent Robots and Systems (Vilamoura, Algarve, Portugal, 7-12 October 2012)*, pp. 1766-1771. doi: 10.1109/IROS.2012.6385947.

[40] S. Mukhopadhyay, C. Wang, M. Patterson, M. Malisoff, and F. Zhang. Collaborative autonomous surveys in marine environments affected by oil spills. In *Cooperative Robots and Sensor Networks 2014*. Koubaa and A. Khelil, eds., Studies in Computational Intelligence Series Vol. 554, Springer, New York, 2014, pp. 87-113. doi: 10.1007/978-3-642-55029-4_5.

[41] C. Samson. Control of chained systems: Application to path-following and time-varying point-stabilization of mobile robots. *IEEE Transactions on Automatic Control*, 40(1):64-77, 1995. doi: 10.1109/9.362899.

[42] E. Sontag. Smooth stabilization implies coprime factorization. *IEEE Transactions on Automatic Control*, 34(4):435-443, 1989. doi: 10.1109/9.28018.

[43] E. Sontag. *Mathematical Control Theory: Deterministic Finite-Dimensional Systems*. Springer, New York, 1998.

[44] E. Sontag. Input-to-state stability: Basic concepts and results. In *Nonlinear and Optimal Control Theory*, P. Nistri and G. Stefani, eds., Springer, Berlin, Germany, 2006, pp. 163-220. doi: 10.1007/978-3-540-77653-6_3.

[45] E. Sontag and Y. Wang. On characterizations of the input-to-state stability property. *Systems and Control Letters*, 24(5):351-359, 1995. doi: 10.1016/0167-6911(94)00050-6.

[46] R. Vinter. *Optimal Control*. Birkhauser, Boston, 2010.

[47] C. Woolsey and L. Techy. Cross-track control of a slender, underactuated AUV using potential shaping. *Ocean Engineering*, 36(1):82-91, 2009. doi: 10.1016/j.oceaneng.2008.07.010.

[48] X. Xiang, L. Lapierre, C. Liu, and B. Jouvencel. Path tracking: combined path following and trajectory tracking for autonomous underwater vehicles. In *Proceedings of the IEEE/RSJ International Conference on Intelligent Robots and Systems (San Francisco, CA, 25-30 September 2011)*, pp. 3558-3563. doi: 10.1109/IROS.2011.6094949.

[49] F. Zhang, J. Chen, Z. Wang and Y. Han. Fault recognition of a 20 mvar statcom main circuit using artificial neural network. In *Proceedings of the 33rd Intersociety Energy Conversion Engineering Confence (Colorado Springs, 2-6 August 1998)*.

[50] F. Zhang, D. Fratantoni, D. Paley, J. Lund, and N. Leonard. Control of coordinated patterns for ocean sampling. *International Journal of Control*, 80(7):1186-1199, 2007. doi: 10.1080/00207170701222947.

[51] F. Zhang, E. Justh, and P. Krishnaprasad. Boundary following using gyroscopic control. In *Proceedings of the 43rd IEEE Conference on Decision and Control (Paradise Island, Bahamas, 14-17 December 2004)*, pp. 5204-5209. doi: 10.1109/CDC.2004.1429634.

[52] F. Zhang, E. Justh, and P. Krishnaprasad. Boundary tracking and obstacle avoidance using gyroscopic control. In *Recent Trends in Dynamical Systems: Proceedings of a Conference in Honor of Jurgen Scheurle*. A. Johann, H-P. Kruse, F. Rupp, and S. Schmitz, eds., Springer, Basel, Switzerland, 2013, pp. 417-446. doi: 10.1007/978-3-0348-0451-6_16.

[53] F. Zhang, A. O'Connor, D. Luebke, and P. Krishnaprasad. Experimental study of curvature-based control laws for obstacle avoidance. In *Proceedings of the IEEE International Conference on Robotics and Automation (New Orleans, LA, 26 April-1 May 2004)*, pp. 3849-3854. doi: 10.1109/ROBOT.2004.1308868.

Vita

Robert Sizemore is a Ph.D. student in the Department of Mathematics at Louisiana State University. In 2010, he received his B.S. degree in Mathematics and his B.S degree in Physics, both from the University of North Carolina at Wilmington. In 2013, he received his M.A. degree from the Department of Mathematics and Statistics at Wake Forest University in Winston Salem, North Carolina. He is a native of Wilmington, North Carolina. He was a Phi Mu Epsilon Physics Honor Society Inductee in 2008. His current interests lie in adaptive and nonlinear control, and his PhD advisor is Prof. Michael Malisoff. He is currently a candidate for the degree of Doctor of Philosophy in Mathematics, which is expected to be awarded in August 2018.